CHALMERS

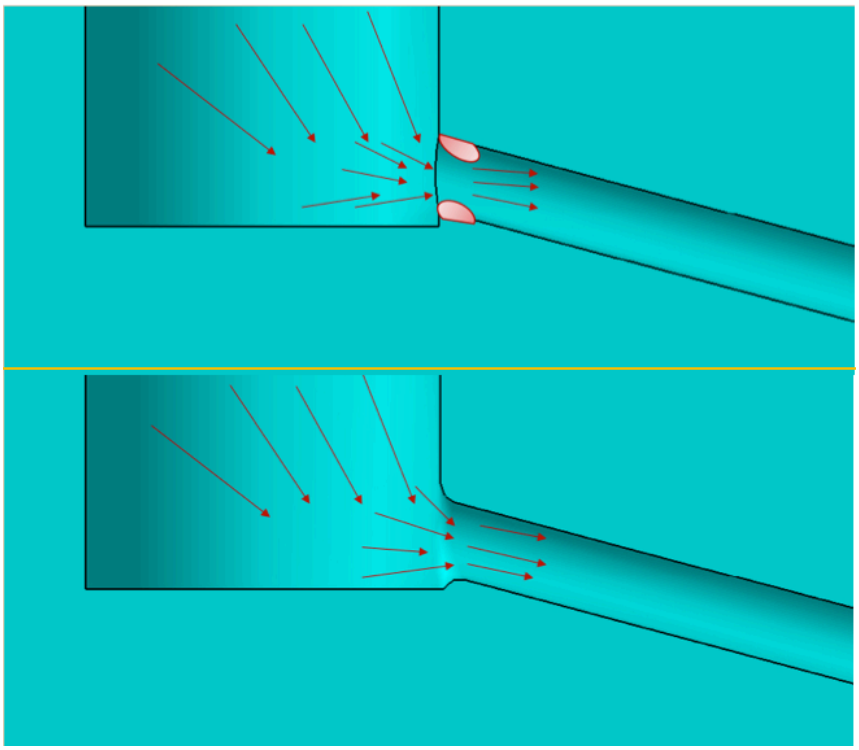

Cavitation in Marine Diesel Applications
Effects of Hydro-erosive Grinding on Flow and Nozzle Geometry

Master of Science Thesis

MOHAMMAD NIKOUEI
Department of Mechanics and Maritime Sciences
Division of Combustion and Propulsion Systems
CHALMERS UNIVERSITY OF TECHNOLOGY
Gothenburg, Sweden 2018

Cavitation in Marine Diesel Applications
Effects of Hydro-erosive Grinding on Flow and Nozzle Geometry

MOHAMMAD NIKOUEI

Department of Mechanics and Maritime Sciences
Division of Combustion and Propulsion Systems

CHALMERS UNIVERSITY OF TECHNOLOGY

Gothenburg, Sweden, 2018

Cavitation in Marine Diesel Applications
Effects of Hydro-erosive Grinding on Flow and Nozzle Geometry

MOHAMMAD NIKOUEI

Department of Mechanics and Maritime Sciences
Division of Combustion and Propulsion Systems
Chalmers University of Technology
SE-412 96 Göteborg
Sweden
Telephone + 46 (0)31-772 1000

Chalmers Bibliotek, Reproservice

Göteborg, Sweden 1999

Cavitation in Marine Diesel Applications
Effects of Hydro-erosive Grinding on Flow and Nozzle Geometry

MOHAMMAD NIKOUEI

Department of Mechanics and Maritime Sciences
Division of Combustion and Propulsion Systems
Chalmers University of Technology

Abstract

In the recent decades, global warming and climate changes have persuaded engineers to improve the design of internal combustion engines in case of pollutant emissions and efficiency. The injection system is one of the main subsystems which can highly affect the quality of mixing process inside the combustion chamber and result in higher efficiency and lower emission. Winterthur Gas & Diesel, which is a manufacturer of marine diesel engines, has come with an idea to improve injection process. The idea is that to remove sharp edges at the entrance of the nozzle orifice and increase its roundness to improve the discharge coefficient and decreasing the vapor volume, which is formed by cavitation.

The roundness of the orifice inlet can be obtained by a hydro-erosive grinding process in which an abrasive fluid with a very high viscosity is extruded through the nozzle orifice and removes the sharp edges and makes a smoother surface. The effect of hydro-erosive grinding on cavitation formation at the entrance of nozzle orifice has been studied in parallel with the following project and the results are published as a licentiate thesis [1].

In the following project, the improvement of the discharge coefficient for three different types of nozzle orifices is investigated by performing several experiments. For this purpose, a literature review has been done to have a suitable theoretical background and to be aware of recent achievements in the relevant fields. The next step is to design and set up test facilities in order to measure the mass flow rate of the nozzle orifices. The system is designed so that water is pressurized to 5 bar by compressed air and is injected through the nozzles over a pre-defined time period. This time period and the pressure inside the pressure vessel are controlled by solenoid valves and a pressure sensor, which are governed by LabVIEW. The discharged mass is weighted and then it is possible to calculate the discharge coefficient.

Before doing the main experiments, several sets of experiments are done to understand the optimum condition where the error is minimum. Then, these conditions are chosen for the main experiments. The mass flow rate for each nozzle is measured five times for eight hydro-erosive grinding levels. In the next step, the average discharge coefficient for each level is calculated and reported in tables and graphs.

From these results, it has been understood that at the initial levels of hydro-erosive grinding, a relatively large increase in the discharge coefficient is observed, while for the next levels its growth continues linearly but with a lower rate. Another achievement of this project shows the behavior of different types of nozzles. The orifices which are placed in a tangential position to the nozzle, need to be grinded more in comparison to the standard nozzle, which its orifice is placed at the center of the nozzle outlet. Inclination in orifice causes decrease in flow resistance. Therefore, hydro-erosive grinding in this case is not as efficient as in the case, where the orifice is perpendicular to the nozzle.

Keywords: cavitation, hydro-erosive grinding, discharge coefficient, injector.

Acknowledgement

This work has been carried out by the Department of Mechanics and Maritime Sciences at Chalmers University Technology in collaboration with Winterthur Gas and Diesel Ltd. and Polytechnic University of Turin.

Hereby, I would like to appreciate my supervisor at Chalmers University of Technology, Prof. David Sedarsky who trusted me and I also appreciate him for his support, help and guidance. In addition, I would like thank my supervisor at Polytechnic University of Turin, Prof. Mirko Barata for his caring and for supporting me.

Thanks to all staff and employees in the Combustion and Propulsion Systems division, especially Reto Balz, who helped me to carry out this project.

Finally, I have to thank my family who supported me to reach to this achievement in my life.

Table of Contents

Nomenclatures

a	Speed of sound
A	Cross sectional area
AE	Absolute error
A_{eff}	Effective cross sectional area
A_{th}	Theoretical cross sectional area
C_a	Area coefficient
C_d	Discharge coefficient
C_v	Velocity coefficient
D	Cross sectional diameter
DP	Pressure drop
F	Friction factor
f_{lam}	Friction factor for laminar flow
G	Gravity acceleration
h_f	Friction head loss
h_m	Minor head loss
h_p	Pump head
h_t	Turbine head
K	Cavitation number
k	Loss coefficient
L	Length of the pipe
m	Mass
M	Momentum
P_a	Ambient pressure
P_{back}	Back pressure
P_{inj}	Injection pressure
P_{sat}	Saturation pressure
P_v	Vapor pressure
Q	Volumetric flow rate
Re	Reynolds number
RE	Relative error
t	Time
u	Flow velocity
u_{eff}	Effective velocity of the flow
u_{th}	Theoretical velocity of the flow
V	Mean flow velocity
x	Mixture quality
Z	Flow altitude
ρ	Density
ρ_{lsat}	Density of liquid at saturation point
ρ_{vsat}	Density of vapor at saturation point
γ	Specific weight
ψ	inverse of sound speed squared

Chapter 1

1. Introduction

1.1 Problem background

Diesel engines for marine applications operate under intense pressure and volume of fuel injection. Therefore, designing the fuel injection system is one of the most challenging works to increase the quality of mixing air and fuel in the combustion chamber to provide higher efficiency and lower pollutant emissions.

Meanwhile, the effect of cavitation and the flow quality at the upstream of the orifice can play an important role in fuel distribution and momentum for a suitable mixing. For this purpose, different arrangements and designs of injector orifices have been designed and tested. The geometry of nozzle holes for automotive diesel engines is much smaller than for marine application. Usually the length of the orifice is about 1 mm with a diameter of 0.1 mm to 0.2 mm for automotive applications, while the nozzle hole geometry for WinG&D engine is 4.5 mm length and the diameter of 0.75 mm.

In the fuel injectors, cavitation mainly occurs at the intersection between the nozzle and the orifice, where there is a sharp edge. It causes deflection of spray formation, reduction of discharge coefficient and worsening of air fuel mixing process. For this reason, hydrogrinding machining can be implemented to increase the roundness of the sharp edges to reduce cavitation and increase the discharge coefficient of the orifice. The important point is to understand the efficiency of the hydrogrinding process and calibrate the process parameters for the desired outcomes.

Hydro-erosive grinding has proven to be a useful process for adjusting internal flow conditions and is widely used in automotive fuel injector designs. This project will advance marine diesel spray diagnostics by implementing hydro-erosive grinding in optical nozzles, which are designed for the Chalmers system and reporting on the methods and observed effects with respect to cavitation and spray morphology. Figure 1.1 can better show the expectation of the flow after performing hydro-erosive grinding on the nozzle and increasing roundness of sharp edges at the entrance of the orifice.

The hydro-erosive grinding (HEG) is applied to optical nozzles which are related to marine engines which are designed by WinG&D. The specialized optical nozzles, injector mounting hardware and hydro grinding rig have been designed before and another system for measuring discharge coefficient is designed and assembled during this project.

1.2 Project structure

This project is a part of a PhD project. The aim of this project is to understand the effect of hydro-erosive grinding on the discharge coefficient of the nozzle orifices. The effect of hydro-erosive grinding on cavitation elimination has been studied during that PhD project and is reported as a licentiate thesis [1].

The following project has been done in four phases:

The first phase is a literature review. During this phase, the most relevant articles have been studied to understand what aspects of the project that is more important and how it is possible to continue research in this field. In addition, it is important to know what the outcomes are of the other researches and compare them with the obtained results. Moreover, it can help to propose a correct methodology for the experiment and analyzing the results and prevent of repetition. In the next chapter some of the most relevant articles and their outcomes are shown.

In the second phase, a methodology has been proposed for the experiment in order to measure the improvement of the flow inside the nozzle after hydro-erosive grinding with small increments.

The next phase has been devoted to the test equipment and hardware setup. The test cell with the all necessary equipment has been designed and all the elements have been mounted correctly together.

Finally, in the last phase, experiments have been done with different nozzles and the project is finished verifying, comparing and analyzing the results. The last three phases are supporting by the theories that has been explained in Chapter 2.

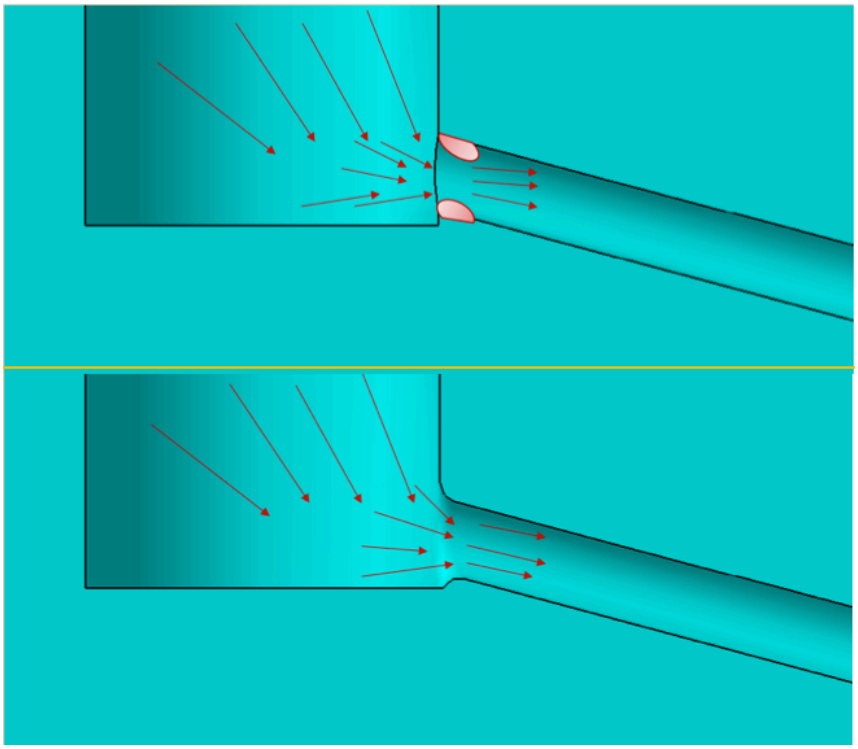

Figure 1.1 Expectation of the flow behavior prior and after hydro-erosive grinding

Chapter 2

2. Theoretical background

2.1 Cavitation

2.1.1 Cavitation theory

At a certain temperature, the pressure at which a liquid boils is called the vapor pressure. If the liquid pressure is greater than the vapor pressure, evaporation at the interface occurs. In opposite, if the liquid pressure becomes lower than the vapor pressure, vapor bubbles will be formed in the liquid. The cavitation number K is a dimensionless parameter which describes flow-induced boiling as

$$K = \frac{P_a - P_v}{\frac{1}{2}\rho V^2} \tag{2.1}$$

where P_a is the ambient pressure, P_v is the vapor pressure, V is the characteristic flow velocity and ρ is the fluid density.

Depending on the geometry, a given flow has a critical value of K below which the flow begins to cavitate. The vapor pressure of the water is plotted in Figure 2.1.

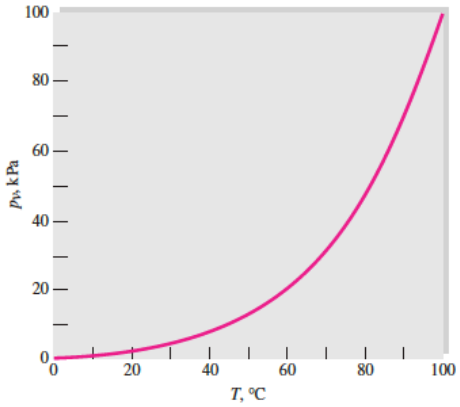

Figure 2.1 Water vapor pressure as a function of temperature [2]

In other words, cavitation is a rapid formation and collapsing of vapor bubbles in a flow. It mainly happens when the static pressure becomes lower than the vapor pressure of the liquid.

Figure 2.2 shows the phase diagram for water. It can be perceived that the phase of any substances depend on temperature and pressure. Let us consider water in the standard environment, which is in liquid phase. Its temperature is 25℃ and its pressure is 1 atm. In order to change its phase to gas, there are two options; it is possible to increase its temperature to 100℃ or to reduce its pressure to 0.006 atm. The second option is called cavitation.

Cavitation usually occurs at edges that are moving fast through a liquid, such as pump impellers or marine propellers. It also can be observed when a sudden change in the cross section of the flow occurs (see Figure 2.3).

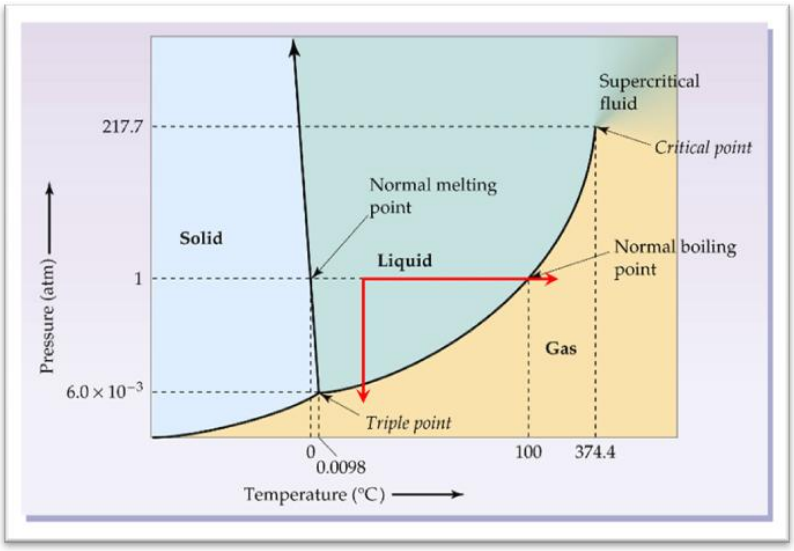

Figure 2.2 Water phase diagram [3]

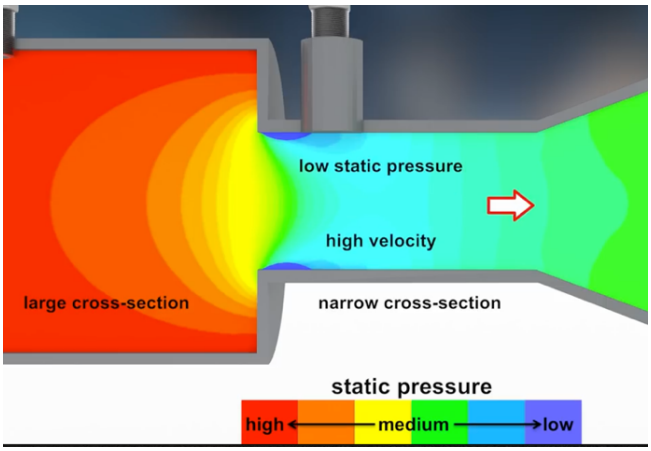

Figure 2.3 Change in flow cross-sectional area causes cavitation [4]

Bubbles which are formed at low pressure regions are transported to high pressure regions. As soon as the pressure exceed the pressure inside the bubbles, they will collapse (see Figure 2.4). Collapsing of these bubbles causes micro cracks on the solid surfaces and in the long term causes major damage.

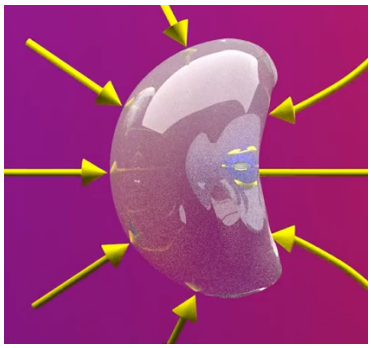

Figure 2.4 Collapsing mechanism for vapor bubbles [4]

Cavitation mainly has three main effects:

1. Cavitation bubbles block flow through reduced cross sections and cause lower effective area.
2. Formation and collapsing bubbles generate noise, which is unpleasant.
3. Finally, continuous cavitation formation causes erosive damages on solid surfaces.

2.1.2 Cavitation effect on diesel injector nozzles

A contribution has been made to understand cavitation effects in diesel injector nozzles through a combined experimental and computational investigation [5]. They have developed a model and solved the equations governing the model. Then, they have set up test facilities and have performed experiments to compare results with the numerical results and validating the model.

They have used barotropic equation of state and assuming fully mixed liquid and vapor and considering compressibility of both phases

$$\frac{d\rho}{dt} = \psi \frac{dP}{dt} \tag{2.2}$$

where ψ is the inverse of the speed of sound squared and is given as

$$\psi = \frac{1}{a^2} \ . \tag{2.3}$$

In the next step, the continuity equation is solved for ρ by using the equation of state

$$\frac{\partial \rho}{\partial t} + \nabla(\rho u) = 0 \, . \tag{2.4}$$

After calculating density, it is time to determine ψ and x which indicates the amount of vapor in the fluid

$$x = \frac{\rho - \rho_{\mathrm{lsat}}}{\rho_{\mathrm{vsat}} - \rho_{\mathrm{lsat}}} \tag{2.5}$$

$$\rho_{\mathrm{vsat}} = \psi \, P_{\mathrm{sat}} \, . \tag{2.6}$$

For the experimental part they used a conventional common rail injection system. They have measured and calculated mass flow rate, momentum flux, effective velocity and flow coefficients.

Their observation about cavitation formation explains that the vapor zone consists of a cyclical process which is formation, growth, collapse and break-off the vapor bubbles. This process has a great influence on velocity profile. The velocity profile is continuously changed depending on the vapor distribution.

In addition, during measurement of mass flow rate in [5], they have found a specific point which is called chocked flow. The mass flow rate proportionally increases with the square root of the pressure drop until a specific point which it is called chocked flow and after this point mass flow rate is stabilized. Moreover, they understood that cavitation will increase as the backpressure decreases. In case of velocity, they noticed that velocity increases by cavitation and this is mainly due to reduction in viscosity and consequently, friction, in presence of vapor.

2.1.3 Cavitation effect on injection velocity

In another article [6], the effect of cavitation on the injection velocity in diesel nozzles has been studied deeply. For this purpose, the continuity equation, the momentum theorem and the energy equation have been used to perform a theoretical analysis about the effect of cavitation on velocity and compare it to a non-cavitating condition. It is believed that under a certain condition, cavitation has the same effect on the mass flow rate $\dot{m}$ and the momentum flux $\dot{M}$. This means that any increase in velocity does not directly depend on the cavitation intensity. It mostly depends on the change in density that is due to the presence of vapor. Therefore, it has been noticed that increase in velocity is related to reduction in viscosity. Lower viscosity causes less friction on the orifice wall. In addition, Reynolds number *Re* will be larger with lower viscosity. Consequently, the turbulence factor of the flow will be increased and affects the velocity profile, which is similar to a “top hat” shape. Moreover,

it is believed that another reason for growth in the flow velocity could be reduction in effective area. It means that a portion of the flow pathway is occupied by vapor volume fractions. Therefore, less area is available for passing the liquid phase.

2.1.4 Effects of geometry on cavitation

A numerical investigation on the effects of the nozzle's geometric parameters on the flow and the cavitation characteristics within injector's nozzle for a high-pressure common-rail diesel engine is reported in another article [7]. In addition to geometrical parameters, the effects of dynamic parameters on cavitation formation have been also investigated. The main parameters include injection pressure, orifice coefficient, ratio of the nozzle length to the orifice diameter and the roughness of the orifice wall. All these parameters have been studied by a three-dimensional simulation.

The main results of these simulations can be explained as follows:

1. Cavitation inside the nozzle starts to be formed as the pressure difference between the inlet and the outlet of the orifice reaches a certain amount. At this point, mass flow rate and consequently, flow coefficients will be reduced considerably, while the flow velocity at the orifice inlet slightly increases. By increasing the pressure difference, mass flow rate and average flow velocity rise, while the flow coefficients remain almost constant.
2. The ratio of the radius of the circular bead to the diameter of the nozzle (*r/D*), can affect cavitation formation. As this ratio increases, mass flow rate and flow coefficients rise until *r/D* equals 0.12; after this point flow coefficients and mass flow rate decrease. In addition, if *r/D* increases up to 0.3, it can quench cavitation by about 45%. Altogether, the optimum design for nozzle and orifice happens when *r/D* is around 0.12.
3. The conicity factor of the orifice is described as the *k-factor*

$$k - factor = \frac{inlet\ diameter - outlet\ diameter}{10}. \tag{2.7}$$

   If it changes from -4 to 4, both mass flow rate and flow coefficient will experience a remarkable increase. In addition, vapor fraction will be decreased significantly. This means that cavitation in conical orifices will be reduced considerably.
4. *L/D* is defined as the ratio of the nozzle length to the orifice diameter. Increase in *L/D* initially will result in growth of the flow coefficient and the mass flow rate, while both of them will be decreased afterwards. However, the peak point for both is not the same; for the mass flow rate the optimum condition happens when *L/D* is equal to 4.06. The peak point for the flow coefficient can be observed when this ratio is equal to 5.36. The results also show that the vapor volume fraction also experiences an increasing and a decreasing trend, which its peak point happens when *L/D* is about 4.06. Therefore, it can be said that the most severe cavitation forms when *L/D* is 4.06. Altogether, the investigation shows that *L/D* equal to 5.36 is the optimum ratio for designing nozzle orifice.
5. The last parameter that has been investigated is the roughness of the orifice wall. Increasing roughness causes a slight rise in mass flow rate and flow coefficient. However, increasing of roughness beyond 10 μm leads to a sharp decrease in both variables. This can be explained by two phenomena. By increasing roughness, friction phenomenon enhances, while cavitation is suppressed. For roughness less than 10 μm, the effect of cavitation suppression is stronger, while for higher roughness friction is increased significantly and worsening both flow coefficient and mass flow rate.

2.1.5 Effects of injection pressure on cavitation

Another investigation has been conducted to find effects of injection pressure on cavitation and spray in marine diesel engines [8]. In this paper, several models have been built numerically to study cavitation under different injection pressures. The main results of this research can be summarized as follows

1. Cavitation will be raised if the injection pressure increases. This is due to inducing higher intensity in pressure fluctuation which causes an increase of the diesel vapor fractions.
2. Since there is no momentum exchange between air and the liquid column at the beginning of the spray, spray penetration is proportional to time. However, the penetration gradually decreases in the middle and

later periods. By increasing the injection pressure, the penetration and the cone angle of the spray increase. Each additional 20 MPa leads to rise in cone angle by 0.8° while in marine applications, cone angle does not change very much respect the time. The range of cone angle for marine application is about 16° to 19°.

3. The fuel is propagated as a shape of liquid column. The structure on the spray edge will come back to the spray body, while the structure of spray head remains unchanged.

2.2. Hydroerosive grinding

2.2.1 Abrasive flow machining (AFM)

There are several parameters which should be considered for abrasive flow machining. Extrusion pressure and number of cycles or timing are the main parameters related to the machine [9]. Rheological properties, type of abrasive, abrasive mesh size, concentration of abrasive and carrier, type of polymer carrier and additives should be taken in to account regarding the abrasive medium.

Abrasive flow machining (AFM) is a machining process to remove the surfaces and make them smoother. In this process a semi-solid medium is used as the abrasive fluid and it consists of visco-elastic polymer reinforced with abrasive particles. This fluid is extruded under high pressure on the surface or through the holes to slightly grind them. In this article the AFM process has been reviewed from four points of view: experimental setup, abrasive media, modeling and optimization and application.

In the case of flow direction, there are three types of AFM. The abrasive fluid can pass in one way only or two ways. There is also another possibility in which the abrasive fluid remains constant and the work piece moves in an orbital manner over it.

According to [9], the most common setups for AFM can be categorized as follows:

- Magneto Abrasive Flow Machining (MAFM);
- Magneto-Rheological Abrasive Flow Finishing (MRAFF);
- Centrifugal Force Assisted Abrasive Flow Machining (CFAAFM);
- Electro-Chemical aided Abrasive Flow Machining (ECAFM);
- Drill Bit Guided-Abrasive Flow Finishing (DBG-AFF);
- Rotational-Abrasive Flow Finishing (R-AFF);
- Ultrasonic Assisted Abrasive Flow Machining (UAAFM)
- Rotational Magneto-Rheological Abrasive Flow Finishing (R-MRAFF)

The most common abrasives are silicon carbide, aluminum oxide, boron carbide and polycrystalline diamond. This process is successfully applied to finish the components with intricate profiles mainly used in automotive, aerospace and biomedical fields.

2.2.2 Effects of hydro-erosive grinding

The study about improving the geometry and quality of a micro-hole fuel injection nozzle by means of hydro-erosive grinding shows that rounding edge of orifice entrance which is made by hydro-erosive grinding, cause reduction in cavitation [10]. However, the hydrogrinding process may leave a negative effect. This process will make a deflection in the nozzle orifice and its shape becomes asymmetric. This effect is called the key-hole effect that should be eliminated from a manufacturing point of view. This usually occurs due to changing the flow direction. It can be prevented by using a fixture to guide the flow in the desired direction.

The author of this paper found that hydro-erosive grinding will affect the engine performance from three aspects. First, it provides a higher discharge coefficient, secondly, a narrow flow band tolerance can be expected and finally, the life-cycle of the nozzle increases and therefore, flow of the fuel does not experience so much change due to wear during actual operation of the nozzle in an engine.

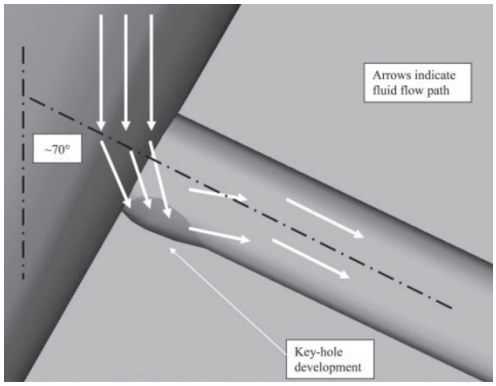

Figure 2.5 Key-hole effect [10]

There are four phases for hydro-erosive grinding:

1. The radiusing of the inlet edge. In this phase, the most significant growth in flow rate can be observed.
2. Polishing. In this phase, the surface finish at the entry and along the hole is improved.
3. The diameter of the hole is being increased.
4. The process is not under control and this can lead to an asymmetrical hole geometry and uneven hole growth.

Another study has been conducted which is about analysis of the combined effect of hydrogrinding process and inclination angle on hydraulic performance of diesel injection nozzles [11]. It has been mentioned that the efficiency of air fuel mixing process depends mainly on the injection pressure and the geometrical characteristics of the injector nozzle. It is due to the fact that these criteria affect the discharge coefficient and cavitation inception. In other words, the Reynolds number is affected by these characteristics. In addition, there are two important parameters that highly influence cavitation formation and intensity. These parameters are the rounding radius of the orifice inlet edge and the orifice inclination angle. A higher rounding level provides smaller pressure loss and lower cavitation inception and this results in a higher discharge coefficient.

The intensity of hydro-erosive grinding can be defined as a percentage, which represents the amount of increase in mass flow rate in comparison with the initial situation, before applying hydro-erosive grinding. In order to analyze the behavior of the flow in terms of pressure losses, effective velocity and effective injection section of the orifice, it is more convenient to use non-dimensional flow coefficients. These dimensionless coefficients consist of the discharge coefficient C_d, the velocity coefficient C_v and the area coefficient C_a. Studies show that increasing rounding radius of the orifice inlet edge will result in higher flow coefficients. This is explained due to decrease in pressure loss because of the less flow detachment and consequently, increase the discharge coefficient.

2.3. Discharge coefficient

2.3.1 Parameters describing the inner nozzle flow

Cavitation in high pressure diesel injectors are usually appears at the entrance of nozzle orifice because of the severe change in the flow direction and the cross-sectional area. This also causes separation of the boundary layer from the wall of the orifice. This phenomenon is called “vena contracta” and a recirculation zone is formed between vena contracta and the wall of the orifice which causes a pressure depression due to flow acceleration.

Since it is too complex to choose proper parameter for characterization the flow, injection pressure and discharge backpressure are used for calculations and analyzing the flow. The difference between injection pressure and discharge backpressure is called drop pressure *DP*

$$DP = P_{\text{inj}} - P_{\text{back}} . \tag{2.8}$$

The velocity and density profile inside the nozzle orifice will not be symmetric under cavitation condition. Therefore, mass flow rate and momentum flux can be described as:

$$\dot{m} = \int u\rho dA \tag{2.9}$$

$$\dot{M} = \int u^2\rho dA \tag{2.10}$$

where $\dot{m}$ is the mass flow rate, $\dot{M}$ is the momentum flux, u is the normal velocity, ρ is the density and A is the cross-sectional area.

The recirculation zone, which forms between vena contracta and orifice wall, virtually causes reduction in cross-sectional area and change in the velocity profile of the flow. Therefore, a smaller geometrical area can be assumed as the cross-sectional area of the flow, which is called effective area A_{eff}. If the velocity is considered constant over the area, it is possible to define also effective velocity u_{eff}. These parameters can be defined as

$$u_{\text{eff}} = \frac{\dot{m}}{\dot{M}} \tag{2.11}$$

$$A_{\text{eff}} = \frac{\dot{m}^2}{\rho\dot{M}} \,. \tag{2.12}$$

In order to calculate the theoretical velocity at the outlet of the orifice, Bernoulli's equation is used between the inlet and the outlet of the nozzle orifice

$$P_{\text{inj}} = P_{\text{back}} + \frac{1}{2}\rho + u_{\text{th}}^2 \;\rightarrow\; u_{\text{th}} = \sqrt{\frac{\Delta P}{\rho}}. \tag{2.13}$$

The discharge coefficient C_d is a non-dimensional parameter, which is obtained by dividing the actual mass flow rate by the theoretical mass flow rate. The theoretical mass flow rate is calculated by using theoretical velocity and assuming constant cross-sectional area and density.

$$C_d = \frac{\dot{m}}{A\,\rho\,u_{\text{th}}} = \frac{\dot{m}}{A\sqrt{2\rho\Delta P}} \,. \tag{2.14}$$

In other words, the discharge coefficient is a criterion to understand losses in the flow. These losses can be divided into two groups. The first one is the loss in velocity and another one is the loss in the area. The former is called velocity coefficient C_v, which relates the effective velocity to the maximum theoretical velocity and the latter is known as the area coefficient C_a. The area coefficient describes the effective area in case of presence of the vapor bubbles in the flow respect the geometrical area. The relation between the flow coefficients can be described as

$$C_d = C_a\,C_v \tag{2.15}$$

$$C_v = \frac{u_{\text{eff}}}{u_{\text{th}}} \tag{2.16}$$

$$C_a = \frac{A_{\text{eff}}}{A_{\text{th}}} \,. \tag{2.17}$$

2.3.2 Effect of back pressure

The influence of back pressure on the flow discharge coefficients of plain orifice nozzle has been studied and the results are available on a journal paper [12]. It explains that the discharge coefficient of a nozzle orifice depends mainly on the flow regime. There are several factors, which define the flow regime, such as Reynolds number *Re*, nozzle geometry, injection pressure difference, back pressure and cavitation.

Usually four types of flow regimes can be seen in a nozzle flow.

1. Turbulent flow (no cavitation)
2. Beginning of cavitation
3. Growth of cavitation
4. Hydraulic flip

In the turbulent flow condition, the discharge coefficient is a function of Reynolds number while in the cavitation flow condition, the cavitation number *K* affects C_d for a sharp-edge inlet orifice.

The results of the experiments show that as the backpressure decreases, cavitation intensity rises. In addition, cavitation formation is affected by nozzle geometry, injection pressure and chamber pressure.

The velocity of the flow varies at different backpressures. This variation will be grater as the square root of the injection pressure difference $\sqrt{\Delta P}$ increases. It means that when $\sqrt{\Delta P}$ increases, the flow losses do not increase linearly. Moreover, the cavitation number *K* also shows an increasing trend when backpressure rises.

Another point can be found in the experiments, which is called the critical cavitation point *Kc*. At this point the discharge coefficient is maximum. In case of $K > Kc$, flow in the nozzle will be in turbulent regime. Therefore, by decreasing Reynolds number, friction factor increases and C_d tends to decrease with rising of square root of cavitation number $\sqrt{K}$.

In case of $K \leq Kc$, the cavitation flow will be appeared. This causes reducing the cross-sectional area of the flow and consequently, increasing resistance to the flow.

Performing experiments with different backpressures and the same pressure difference shows that the flow regime depends on backpressure. In the case of turbulent flow regime, the nozzle flow and C_d are mainly depend on Reynolds number, so that C_d increases proportionally to *Re*

$$C_d = \frac{Re}{1465.8\frac{l}{d} + 1.008\,Re} \tag{2.18}$$

where *l* is the orifice length and *d* is the orifice diameter.

At each backpressure, when *Re* exceeds the first critical *Re*, nozzle flow regime will be converted to the cavitation flow regime. In this case, there is a linear relationship between the discharge coefficient and the cavitation number

$$C_d = 0.266 + 0.497\sqrt{K}\,. \tag{2.19}$$

The discharge coefficient will be remained approximately constant until the Reynolds number increases further to the second critical Reynolds number.

2.4 Fluid mechanics theory

2.4.1 Mass flow rate measurement

In order to calculate the discharge coefficient, it is necessary to measure the mass flow rate. There are different devices available for this purpose; however, the simplest method is collecting the discharging fluid over a specific time and measuring the weight of the collected fluid. The accuracy of this method depends on the timer, the collecting strategy and the device, which is used for measuring weight

$$\dot{m} = \lim_{\Delta t \to 0} \frac{\Delta m}{\Delta t}. \tag{2.20}$$

2.4.2 Velocity measurement

The mass flow rate can be also calculated as

$$\dot{m} = \rho Q = \rho V A \tag{2.21}$$

where Q is the volume flow rate, ρ is the mass density of the fluid, v is the flow velocity or the mean velocity and A is the cross-sectional area.

By measuring mass flow rate and using Equation (2.21), it is possible to simply calculate the mean velocity of the flow. The velocity can be used later to calculate flow losses in the system

$$V = \frac{\dot{m}}{\rho A} . \tag{2.22}$$

2.4.3 Pressure loss

In any hydraulic system there is friction between the fluid and the wall of the system components which consist of pipes and connectors. Presence of friction cause reduction in pressure, velocity and flow coefficients flow which is called loss. There are two type of losses in a hydraulic system: the first one happens only due to friction between the flow and the wall of the pipe or duct while the second type occur due to change in the flow direction or cross-sectional area. The former is called major loss and the later is known as minor loss.

The effect of friction on the flow can be taken into account in energy equation. This equation is for incompressible flow through ducts or pipes when a turbine or pump are included. However, pumps or turbines may not be existing and in that case their corresponding terms will be equal to zero

$$\left(\frac{p}{\gamma} + \frac{V^2}{2g} + z\right)_{\text{in}} = \left(\frac{p}{\gamma} + \frac{V^2}{2g} + z\right)_{\text{out}} + h_f - h_p + h_t \tag{2.23}$$

where P is the pressure, γ is the specific weight, g is the gravity, V is the flow velocity and h is the head.

The head loss is always positive which means that friction loss is always positive in reality. Every term in this equation is a length, or head. The terms in parentheses are for upstream and downstream of the flow. A pump provides energy to the flow so it should increase the energy of the upstream while a turbine consumes energy of the fluid to provide work. Friction losses have the same mechanism of turbine but the consuming energy by frictions wastes and is not converted to work. Therefore, pump head must be subtracted from the right side (downstream) of the equation and turbine and friction head must be added to them.

2.4.3.1 Head loss

In a real hydraulic case, flow is exposed to friction and slightly looses its energy. This amount of energy can be defined as a reduction in the height of hydraulic grade line (HGL). The following equation can be used in order to calculate losses in pipes

$$h_f = f \frac{L}{d} \frac{V^2}{2g} \tag{2.24}$$

where L is the length of the pipe, d is the pipe diameter, V is the flow velocity, g is the gravity acceleration and f represents the friction coefficient.

2.4.3.2 Friction factor

In Equation (2.24), f is called friction factor, which is a function of Re, wall roughness and duct shape. The roughness height of the pipe wall (ε) is mostly important in turbulent flow. Therefore, for laminar flow through a circular pipe, friction factor depends only on Reynolds number:

$$f_{lam} = \frac{64}{Re} . \tag{2.25}$$

In case of turbulent pipe flow, calculation of friction factor will be too complex. Moody chart is the simplest method to estimate friction factor in a turbulent pipe flow. This chart can be used both circular and non-circular pipes and also for open-channel flows. The accuracy of this chart is approximately 15 percent.

2.4.3.3 Minor or local losses

As it mentioned before, in addition to the friction loss through the pipes, there may be other type of losses which are caused by the the following reasons

- Pipe entrance or exit
- Sudden expansion or contraction
- Bends, elbows, tees, and other fittings
- Valves, open or partially closed
- Gradual expansions or contractions

Although these losses are called minor but sometimes they may cause greater loss in comparison with a major loss in a long pipe. The complexity of flow pattern in fittings and bends has made it difficult to calculate losses theoretically. Therefore, most of the minor losses usually are measured experimentally and correlated with the pipe flow parameters. Sometimes, these data are mostly related to the manufacturer design, especially for valves. However, for elbows and components which cause change in cross-sectional area there are several experimental graphs which can be used to estimate the minor losses for these components.

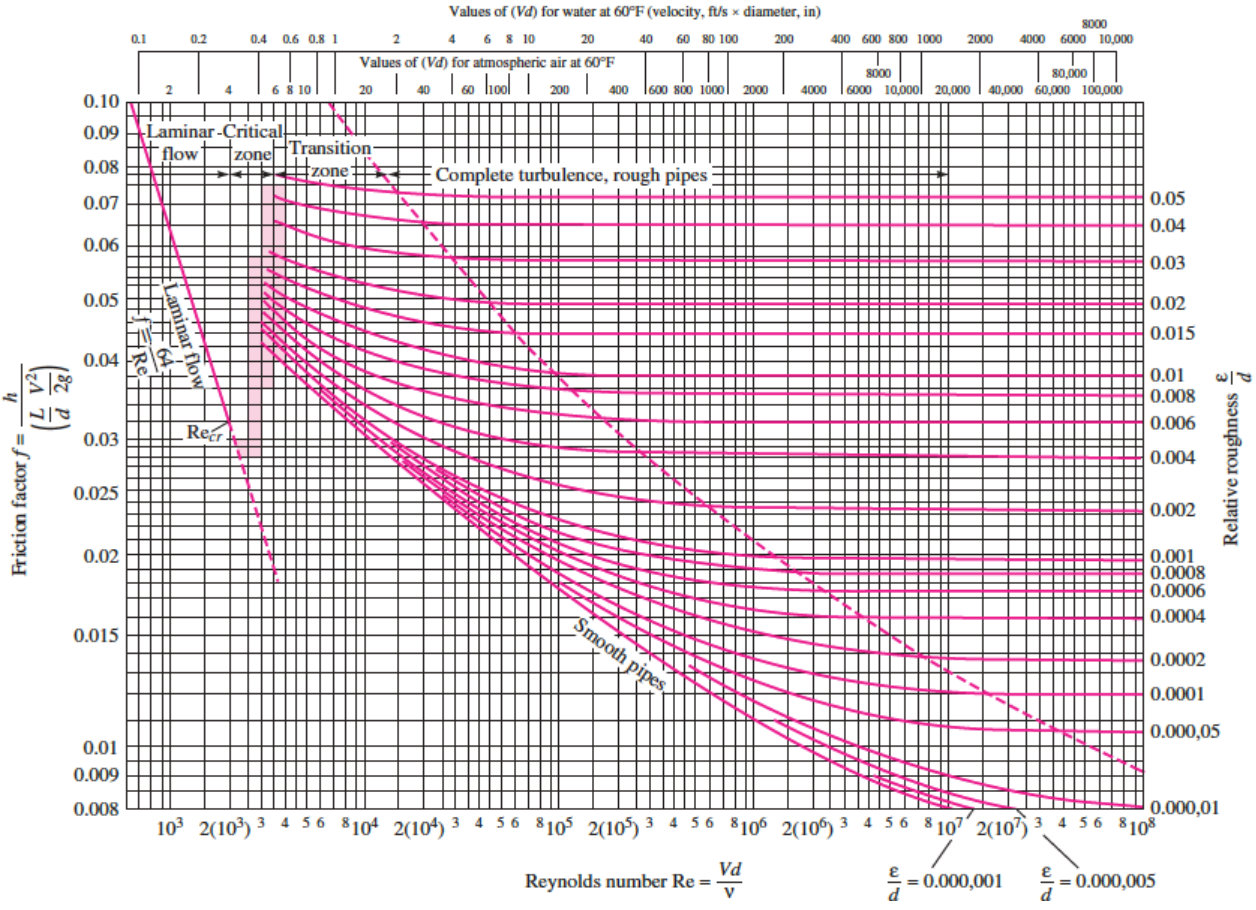

Figure 2.6 Moody chart [2]

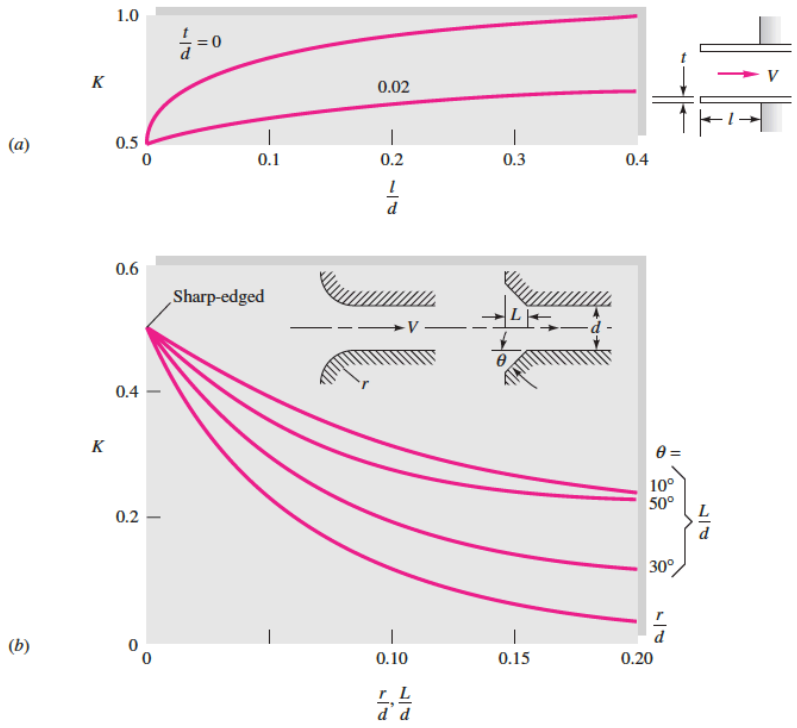

Figure 2.7 Entrance and exit loss coefficients: (a) reentrant inlets; (b) rounded and beveled inlets [2]

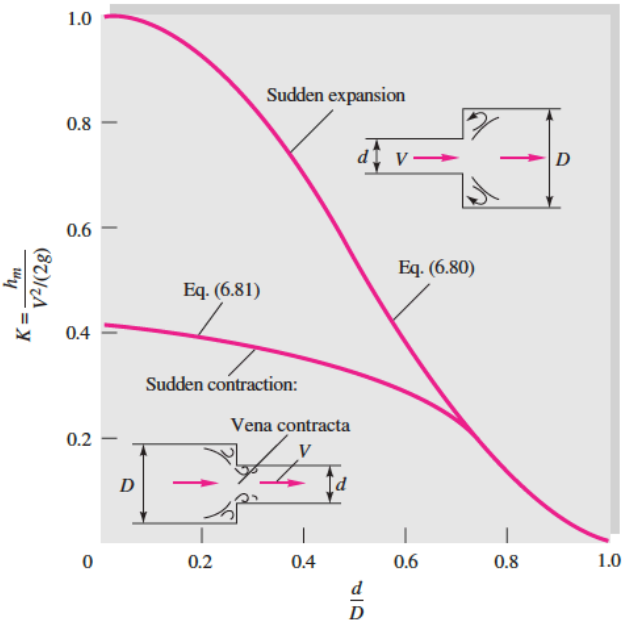

Figure 2.8 Sudden expansion and contraction losses [2]

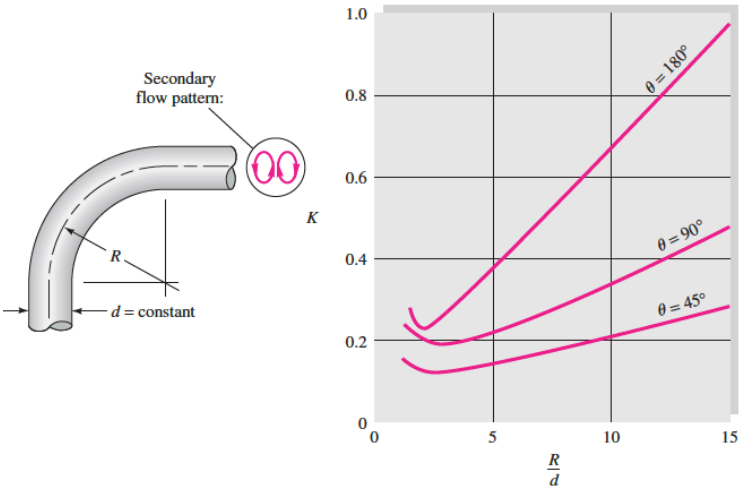

Figure 2.9 Resistance coefficients for bends [2]

The minor losses usually are represented as the ratio of the head loss to the velocity head, which is called the loss coefficient k. It is a dimensionless number

$$k = \frac{h_m}{\frac{V^2}{2g}} = \frac{\Delta P}{\frac{1}{2}\rho V^2} \tag{2.26}$$

where h_m is the minor losses, V is the velocity, g is the gravity acceleration, ΔP is the pressure difference and ρ is the fluid density.

A hydraulic system may have several minor losses. Total loss of the system can be calculated by summing all the losses of the system

$$\Delta h_{\text{tot}} = h_f + \sum h_m = \frac{V^2}{2g}\left(\frac{fL}{d} + \sum K\right). \tag{2.27}$$

Equation (2.27) is valid only in case where the cross-sectional area is constant. Otherwise, the term V (velocity of the fluid) will be changed and the minor losses must be summed separately.

2.5 Error estimation

2.5.1 Absolute and relative error

It is never possible to claim that a measured variable has no error because a lot of factors affect the accuracy of an experiment. For instance, operator error, error due to accuracy, limitation and calibration of the measuring devices cause uncertainty in measuring a physical parameter.

The real amount of each parameter is the amount that is measured by the most precise device until now or is obtained by theoretical calculation. Absolute error means the absolute difference between the measured amount and the real amount of a parameter and it is always mentioned with a unit. Relative error is equal to absolute error divided by the real amount. Relative error is a dimensionless number and can be expressed in percent:

$$AE = |\,Real\ amount - measured\ amount| \tag{2.28}$$

$$RE = \frac{|\,real\ amount - measured\ amount|}{real\ amount} * 100\,. \tag{2.29}$$

2.5.2 Theoretical error

Sometimes there are other kind of parameters which are not measured. They are calculated by equations or theoretical relations with the other variables which are measured. In order to calculate theoretical error of a parameter, which is a function of other variables, Equation (2.31) can be used. This error (Δy) has the same unit of the main parameter:

$$y = f(x_i) \;\; i = 1,2,\dots,n \tag{2.30}$$

$$\Delta y = \sqrt{\sum_{i=1}^{n} \left(\frac{\partial f}{\partial x_i}\right)^2 (\Delta x)^2} \; . \tag{2.31}$$

Chapter 3

3. Test setup

In order to understand the effect of hydroerosive grinding on cavitation and the discharge coefficient of a nozzle, a methodology should be proposed for the experiments. The next step is to design and set up test facilities.

3.1 Theory of the experiment

The experiment is done in two main phases. The first phase is measuring the discharge coefficient of the nozzle orifice and the second phase is applying hydro-erosive grinding on the nozzle and again measuring its discharge coefficient. This process repeats for several times until cavitation vanishes and the variations in the discharge coefficient tend to become constant. In other expression, a calibration is performed to understand the ratio between the amount of hydro-erosive grinding on the flow in the nozzles.

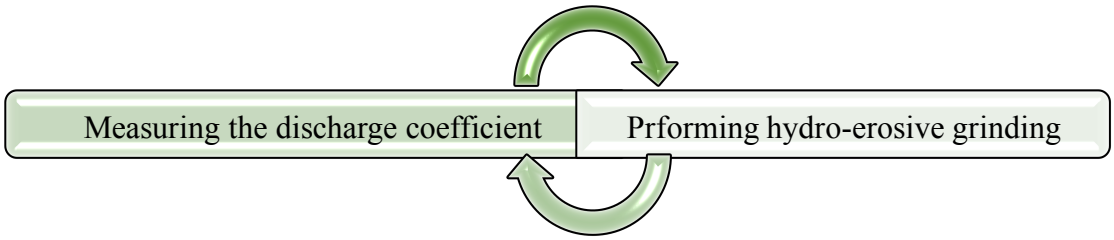

Figure 3.1 Process of the experiment

For the first phase, the working fluid is deionized water. The water must be pressurized in order to move through the system.

3.2 Requirements

According to the theory of measuring the discharge coefficient, which has been explained in Chapter 2, a system has to be designed so that can provide a uniform flow under a constant pressure. Then, the mass flow rate is calculated by measuring the weight of the outgoing fluid over a specified time. This system has been designed by CATIA and then has been set up.

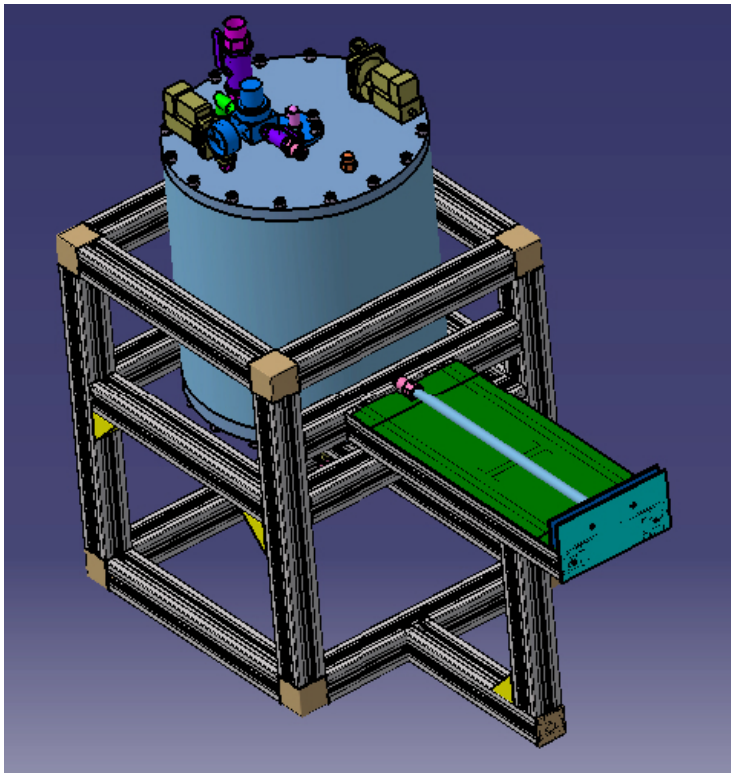

Figure 3.2 Designed test cell

The system consists of a pressure vessel, three solenoid valves, a pressure regulator, a pressure sensor, a safety valve, several ball valves and several plumbing connectors. The two solenoid valves, the pressure sensor and the pressure regulator are mounted on the system to provide a constant pressure with marginal error. Another solenoid valve is used to provide flow motion for a specific time period. To obtain a uniform flow, a relatively long pipe is attached to the third solenoid valve and the nozzle clamp is mounted on the other end of the pipe. The connection between the pressure vessel and the pipe is done by a flexible hose.

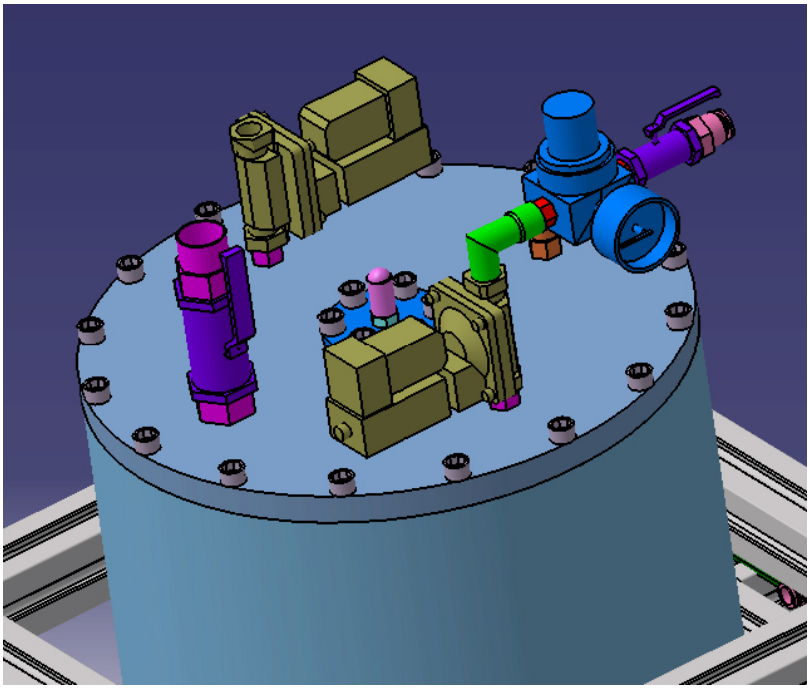

Figure 3.3 Test cell equipment which are mounted on the top of the pressure vessel

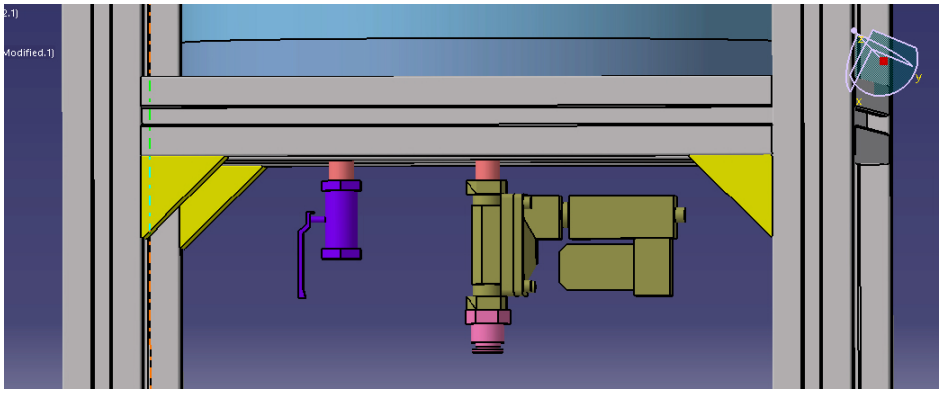

Figure 3.4 Test cell components which are mounted in the bottom of the pressure vessel

Another system is required in order to apply hydro-erosive grinding on the nozzles. In fact, this system is a hydraulic piston which is fixed on a structure. It pressurizes abrasive fluid for extrusion through the nozzle for a specific time period.

3.3 System specification

3.3.1 Hydro-erosive grinding system

The system is designed so that can provide up to 100 bar pressure. It is programmed to pressurize the abrasive fluid between 10 s to 90 s with the increments of 10 s. A 1.5 kW electric motor pressurizes hydraulic oil to apply force on the piston to push the abrasive fluid through the nozzle. The nozzle is mounted on the top of the piston using a clamp. The abrasive fluid contains solid particles which can remove surfaces from a material when passing over a surface with high friction. This high friction is provided by a high viscous fluid. Figure 3.5 shows some abrasive fluid which is used for hydro grinding the nozzles.

Figure 3.5 Abrasive fluid

3.3.2 C_d Measurement

The system which is designed to measure the discharge coefficient of the nozzles is suitable to operate up to 30 bar in terms of pressure and safety. The solenoid valves and pressure sensor are programmed by LabVIEW. A data acquisition device and a relay make the connection between these devices and the computer. The water inside the pressure vessel is pressurized by an air compressor which its maximum discharge pressure is about 6 bar. The back pressure for all the experiments is considered equal to the ambient pressure.

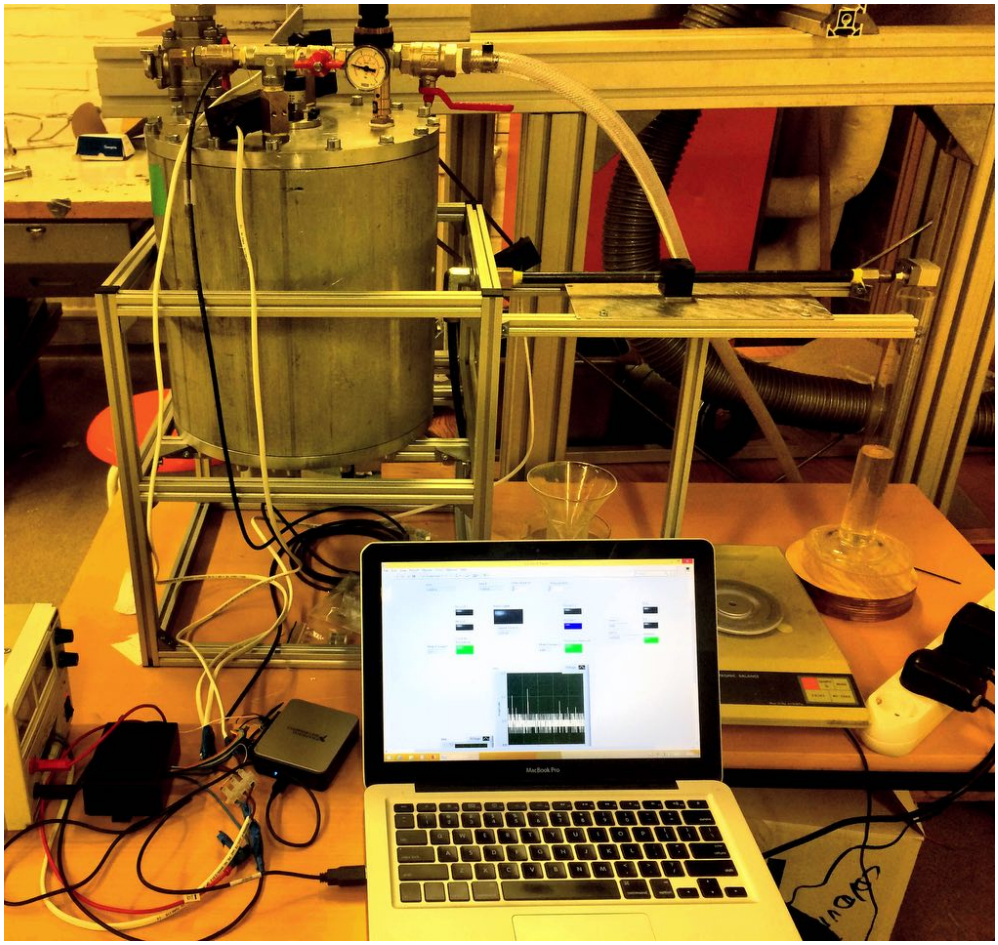

Figure 3.6 The system for measuring discharge coefficient

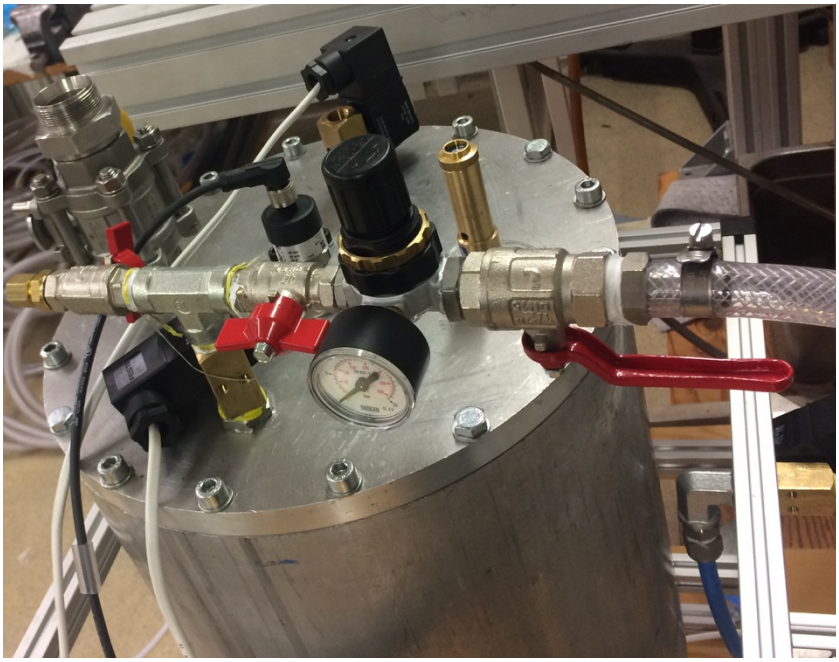

Figure 3.7 Equipment on the upstream of the flow

3.3.3 Nozzles

Since the main purpose of the project [1] is the investigation of cavitation, nozzles should be transparent to facilitate the observation of the cavitation forming. Therefore, the same nozzles are used to measure their discharge coefficient under different hydro-grinding levels. They are made of PMMA polymer which gives a high strength close to metal materials. Nevertheless, for this experiment, a stainless steel nozzle is also used to have a comparison.

From the geometry point of view, there are three types of nozzle orifices; centered and straight (Type 101), tangential to the nozzle and straight (Type 104) and finally, centered but with inclination (Type 105). The front, left and top view of the nozzles and their related photos are shown in Figure 3.8 to Figure 3.10.

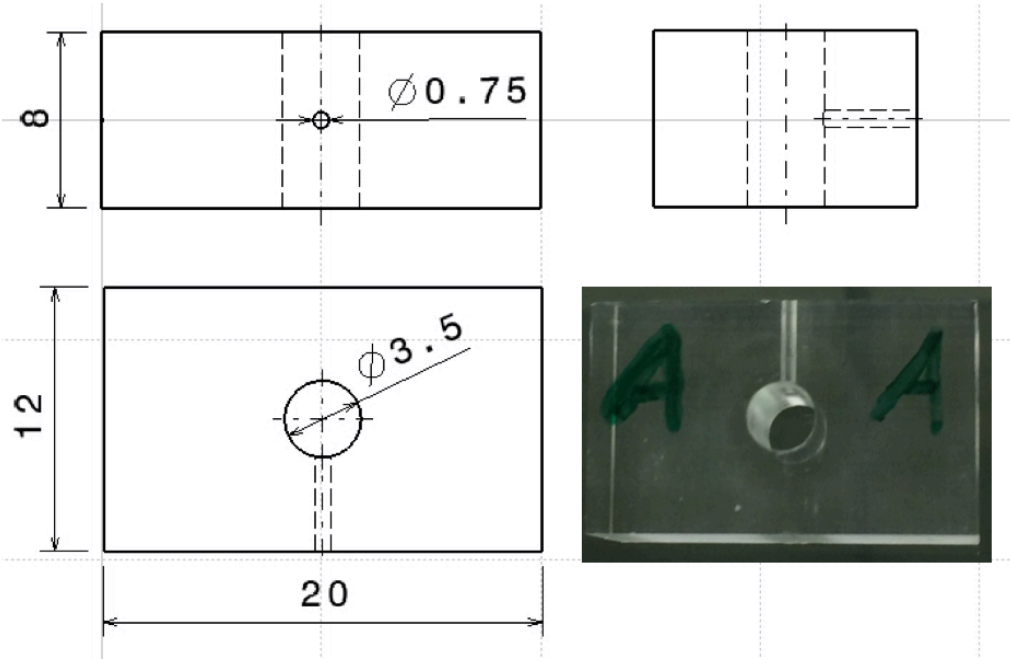

Figure 3.8 Nozzle 101; its orifice is placed on center with no inclination

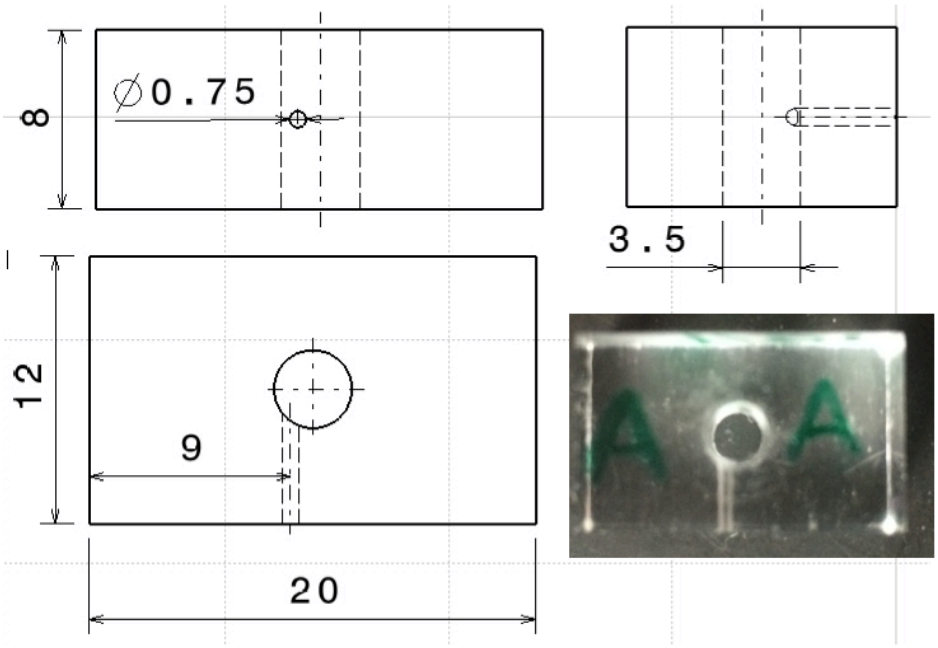

Figure 3.9 Nozzle 104; its orifice is placed tangential to the nozzle with no inclination

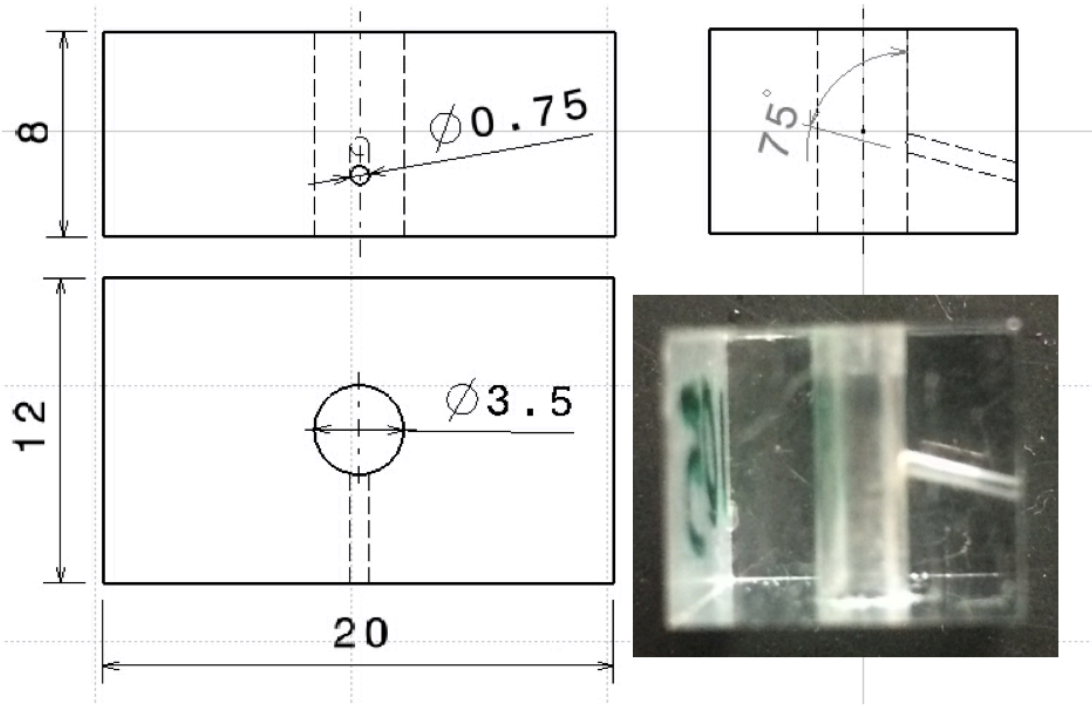

Figure 3.10 Nozzle 105; its orifice is placed on center with inclination

3.3.4 Clamps

The nozzles have to be mounted on both systems so that there will be no leakage. In addition, the flow must be guided properly to enter from one end of the nozzle and exit from the nozzle orifice. Therefore, a clamp should be used to close one end of the nozzle and convert the open end to threads for connecting nozzle to the pipe in an acceptable manner.

The designed clamps for measuring discharge coefficient consists of two parts which are fixed together by four screws. Both ends of the nozzle are sealed by O-rings which are mounted on the clamp parts.

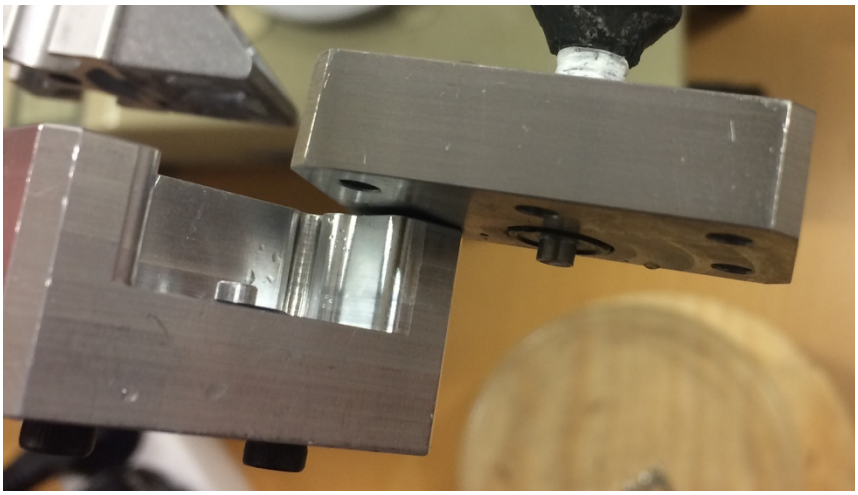

Figure 3.11 Clamp to fix the nozzle to the Cd measurement system

For the hydro-grinding system, the clamp consists of only one part and it fixes the nozzle on the head of the hydraulic cylinder.

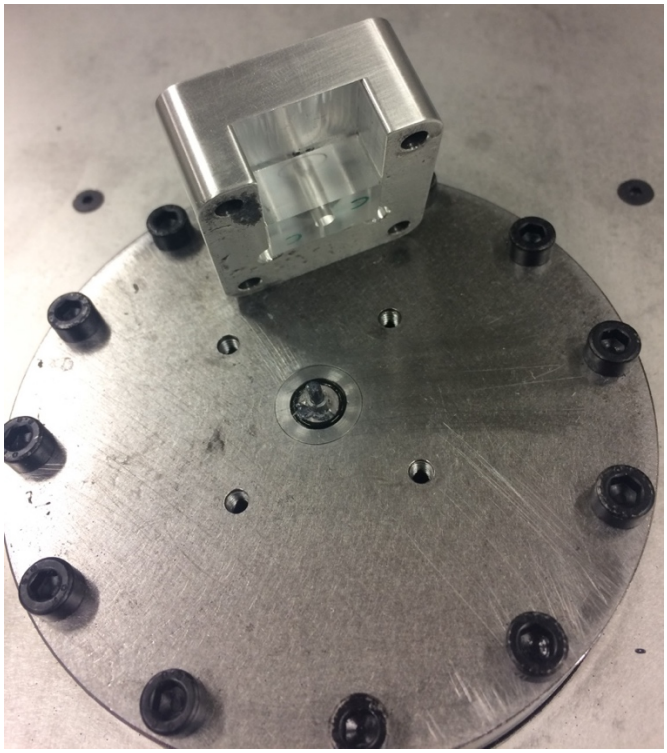

Figure 3.12 Clamp to fix the nozzle on hydro-grinding rig

3.4 Test procedure

3.4.1 Procedure

As mentioned before, first step is to measure the discharge coefficient of a nozzle, then apply hydro-erosive machining and again measure its discharge coefficient. This process continues until cavitation vanishes.

Before starting experiments, there is an important question; how the variables should be chosen for the experiments? These variables are timing period and the pressure of the water. To answer this question, a separate set of experiments is performed to obtain the best answer.

Table 3.1 Selected pressure and time periods for pre-experiments

Pressure [bar]	**3**				**4**				**5**			
Time Period [s]	10	15	20	30	10	15	20	30	10	15	20	30

As can be seen in Table 3.1, three different pressures are chosen and the experiments are done under these pressures for four different timing period. In order to make sure about the accuracy and deviation of results, the experiments are done five times for each condition. In other expression, the discharge coefficient is calculated for sixty times totally.

In the next step, it is important to find the best condition which gives the most accurate and least deviations. However, before that it is necessary to calculate uncertainties and estimate possible errors.

3.4.2 Calculation of Cd

As was explained before in Chapter 2, the discharge coefficient is the ratio between the actual mass flow rate to the theoretical mass flow rate. It can be calculated as

$$C_d = \frac{\dot{m}}{A\sqrt{2\rho\Delta P}}. \tag{3.1}$$

The variables of the equation are defined as the follows:

- $\dot{m}$**:** This indicated actual mass flow rate. In order to calculate $\dot{m}$, the discharged water is collected over a specified time (Δt). Then the collected water is weighted. By dividing the weight of the water (Δm) over the specified time, mass flow rate will be obtained as

$$\dot{m} = \frac{dm}{dt} \approx \frac{\Delta m}{\Delta t}. \tag{3.2}$$

- A**:** It is the cross-sectional area of the orifice. For these nozzles the orifice diameter is 0.75 mm and therefore, cross-sectional area can be calculated.

- ρ: The density of the water is considered constant with the amount of $1 \pm 0.02\ \mathrm{g/cm^3}$.

- ΔP**:** Pressure difference between upstream and downstream of nozzle orifice. The pressure sensor on top of the pressure vessel gives information about the relative pressure inside the tank. Since back pressure is equal to the ambient pressure, therefore, the reported pressure by the sensor can be considered as the pressure difference. However, water will experience loss in its pressure during its pathway to the orifice. These losses should be calculated to have better estimation about the pressure difference.

Pressure loss: As it explained before, there are two kinds of losses in a system: friction loss and local loss. Friction losses are caused by friction in two pipes. One of the has the length of 1 m and another one is 0.45 m. In order to calculate friction loss, first of all the velocity of the fluid is calculated by Equation (3.3)

$$V = \frac{\dot{m}}{\rho A}. \tag{3.3}$$

Then, Reynolds number is calculated to understand flow regime by Equation (3.4)

$$Re_D = \frac{\rho V D}{\mu} = \frac{V D}{\upsilon}. \tag{3.4}$$

Since the flow regime is laminar, the friction factor can be obtained by Equation (3.5)

$$f = \frac{64}{Re} \tag{3.5}$$

Finally, friction head is calculated by Equation (3.6)

$$h_f = f\frac{L}{d}\frac{V^2}{2g}. \tag{3.6}$$

The next step is to calculate minor or local losses. There are, two sudden contractions one bend and one solenoid valve prior to the nozzle entrance. The loss coefficient of the valve is given by the manufacturer while the loss coefficient for the bend and contractions must be estimated by using Figure 2.8 and Figure 2.9.

3.4.3 Accuracy and error estimation

As mentioned in Chapter 3, there are two kinds of errors in addition to operator error. The first type is due to accuracy of a device and the second one is the theoretical error, which are called secondary errors.

3.4.3.1 Primary errors

Primary errors are due to lack of accuracy of the measuring device or delay in operational devices. They are listed in Table 3.2.

Table 3.2 Primary errors

Variable	Error	Unit
Pressure	± 0.2	bar
Time	± 0.04	s
Weight	± 0.001	g
Density	± 0.02	g/cm^3

- **Pressure**

As mentioned before, a pressure sensor, a pressure regulator and two solenoid valves (one for inlet and another for vacuum) are used to provide a constant pressure. However, these devices have operational error. The main error is due to delay in opening and closure of solenoid valves and accuracy of the pressure sensor.

- **Time**

Time error is related to two factors. First, it is related to delay in opening and closure of solenoid valve which controls water flow. Second, it is due to delay in LabVIEW and data transferring from computer to the system.

- **Weight**

There are two scales to measure the weight of discharged water. The first one has the capacity of 310 g and its accuracy is 0.001 g. The capacity of the second one is higher than 1 kg but its accuracy is 1 g and therefore, it is not acceptable. The effort is to limit total weight of the discharged fluid to 310 g.

- **Density**

Density of water depends on pressure and temperature. Since there is no accurate equipment to measure the volume of discharged water, density is assumed to be constant with the amount of 1 g/cm^3 and maximum error is estimated about $\pm 0.02\ g/cm^3$.

3.4.3.2 Secondary error

The secondary errors come from calculation which the parameters of a formula have different error ranges.

Table 3.3 Secondary errors

Variable	Function of	Error	Unit
Mass Flow Rate	m , t	variable	m/s
Discharge Coefficient	$\dot{m}, P, \rho$	variable	-

- **Mass flow rate**

Mass flow rate is explained as a derivation of mass over time. Therefore, it is a function of mass and time. In order to calculate error in mass flow rate it is recommended to use Equation (3.2).

- **Discharge coefficient**

In order to estimate error in calculation of discharge coefficient, Equation (2.30) is used. According to Equation (3.1), discharge coefficient is a function of mass flow rate, pressure and density.

Figure 3.13 shows the accuracy of different conditions in percent. 8th and 12th sets have considerably higher inaccuracy. The reason is related to the accuracy of weight measurement. There are two devices to measure weights. One of them has the accuracy of 1 mg but the maximum capacity is 310 g. In these two cases, the weight of water and its storage bottle exceed 310 g therefore, it is needed to measure weight by the scale which has less accuracy.

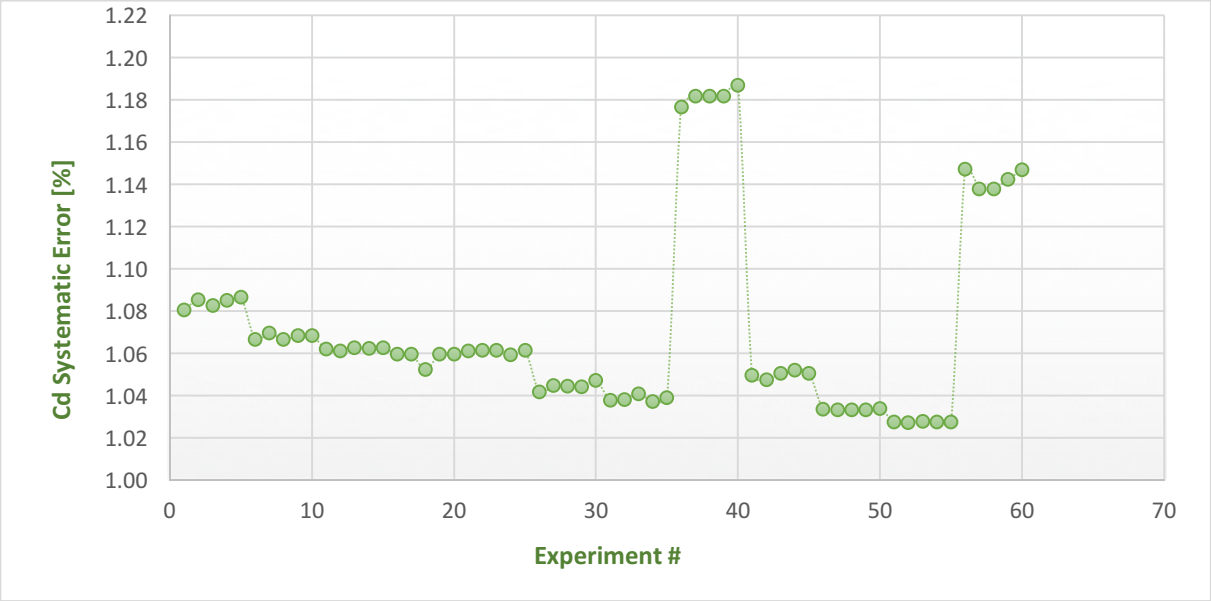

Figure 3.13 Error in measuring discharge coefficient by different experiments

It is obvious that the 11th set of the experiments will provide the most accurate results in comparison with the other conditions. Nevertheless, it would not be the best choice because in this case, the capacity of the scale reaches to its maximum. Therefore, it is not possible to measure the weight of the water after performing hydro-erosive grinding. This problem also may occur for the 10th set. Altogether, it seems that the 9th set of conditions, which is at 5 bar pressure and 10 s time period, will be the best choice. It should be mentioned that operating under higher pressure is preferred because the possibility of cavitation formation increases as the pressure rises.

After choosing the best condition for the experiments, it is time to start measurements. There are five transparent nozzles which are marked with the letters A to E and a stainless steel nozzle. All of them belong to the first type of nozzles, that means all of them have the centered and straight orifice. For the other types of nozzles (104 and 105) There are three transparent nozzles which are marked with the letters A to C.

Figure 3.14 Five transparent nozzle and one metallic nozzle are ready for experiments

Experiments start with measuring the discharge coefficient of all the nozzles. Then, all of them are mounted on hydro-erosive grinding rig to push abrasive fluid through them for 20 s under the pressure of 90 bar. After cleaning the nozzles, they are ready for measuring their discharge coefficient again. According to cavitation observation in these nozzles in [1], this process should be repeated for seven times or 140 s of hydro-erosive grinding. The reason is that cavitation will be vanished after 120 s of hydro-erosive grinding under the same situation [1]. Nevertheless, a step further is performed to ensure about the behavior of variations in discharge coefficient.

3.5 Results

The results for the three kinds of nozzles are summarized in three tables and three graphs. The discharge coefficient related to hydro-erosive grinding time are shown in a graph while the average discharge coefficient for all the same kind of nozzles can be seen on a table.

3.5.1 Centered and straight orifice (Nozzle 101)

As explained before, this kind of nozzles are the simplest one which has straight and centered orifice. The experiment has been done on six nozzles of this type. Five nozzles which are marked with the letters A to E, are made of PMMA polymer and another nozzle is made of stainless steel which is more stiff in comparison with the other nozzles and it is marked with the letter M.

The trend of increase in the discharge coefficient is almost similar in all the nozzles. All of them roughly have the same discharge coefficient before hydro-erosive grinding. After having 20 s of hydro-erosive grinding, a significant rise in discharge coefficient is observed for all of the nozzles. However, it can be seen that nozzle A has significantly higher increase and nozzle M has the lowest increase. The first problem may be due to lack of calibration of hydro grinding rig or manufacturing error. Since the hardness of stainless steel is higher than PMMA, it is reasonable to see lower change in discharge coefficient for nozzle M in comparison with the other nozzles. Anyway, since the trend in discharge coefficient of other four nozzles are similar and roughly coinciding the average, it is possible to neglect nozzle A.

Table 3.4 Average discharge coefficient for different hydro grinding levels for nozzle 101

HEG time	0	20	40	60	80	100	120	140
AVG Cd	0.589	0.725	0.738	0.750	0.763	0.775	0.789	0.803
Improvement	0	23%	25%	27%	30%	32%	34%	36%

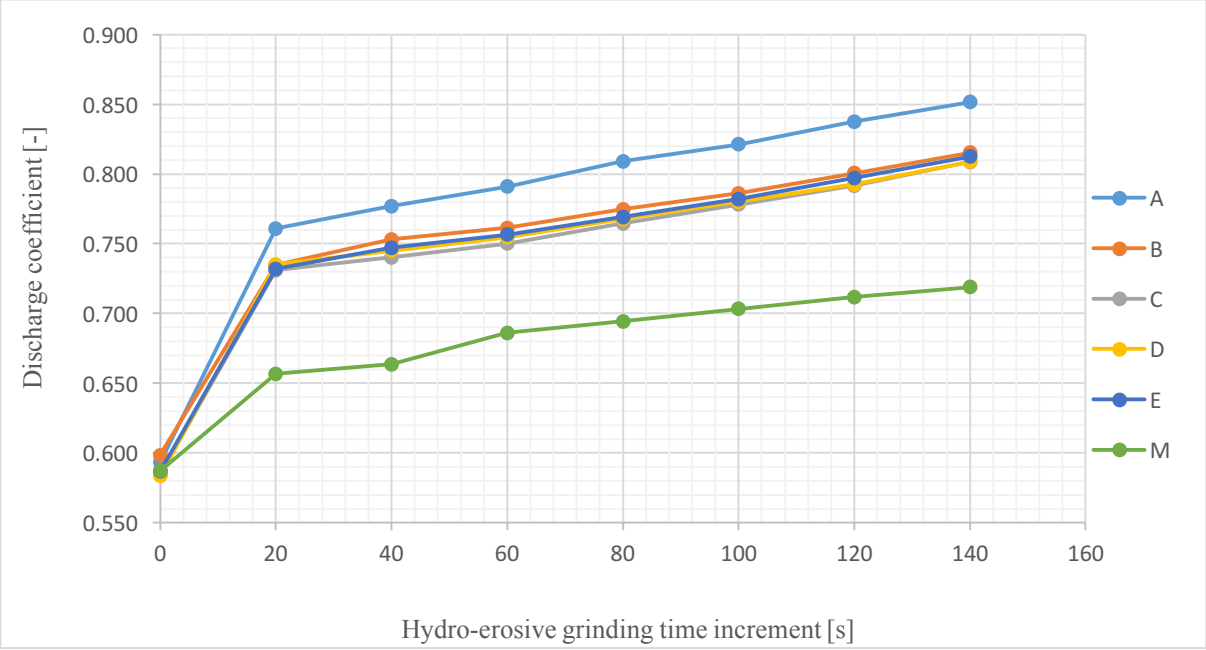

Figure 3.15 Measured discharge coefficient for different hydro-erosive grinding levels for nozzles type 101

The trend of the discharge coefficient with hydro-erosive grinding includes a large increase and a linear increase, that happens after 40 s of hydro-erosive grinding. It is important to mention that hydro-erosive grinding can affect the geometry of the orifice from two different ways; it removes the sharp edge at the entrance of the orifice, it removes a very thin layer of the orifice surface. The latter makes the surface of the orifice smoother and also increase its diameter although it is negligible.

3.5.2 Tangential and straight orifice (Nozzle 104)

The second type of nozzles which are distinguished with the code of 104 and have straight and offset orifice. There are three nozzles of this type which are marked with the letters A to C and made of PMMA polymer.

The trend of increase in discharge coefficient by hydro-erosive grinding is slightly different in comparison with type of 101. In this case, a significant rise in discharge coefficient occurs after 20 s. After 40 s, the growth is smaller than the first grinding step but it is still higher than he next steps. After this point, the rate of increasing remains almost constant and it the trend is linear.

It seems that the effect of sharp edges is more considerable for this kind of nozzles compared to the previous type.

Table 3.5 Average discharge coefficient for different hydro-erosive grinding levels for nozzle 104

HEG time	0	20	40	60	80	100	120	140
AVG Cd	0.579	0.687	0.732	0.751	0.767	0.783	0.797	0.812
Improvement	0	18%	26%	30%	32%	35%	38%	40%

3.5.3 Centered and angled orifice (Nozzle 105)

The last three nozzles which contain angled and centered orifice are known as type 105. These nozzles are marked with the letters A to C and made of PMMA Polymer.

As can be seen in Figure 3.17, after the first hydro-erosive grinding process, the discharge coefficient of all the nozzles highly increase. After this point the rate of increase remains constant and it is similar to type 101. It can be described as a significant rise and a constant growth after 20 s of hydro-erosive grinding.

Table 3.6 Average discharge coefficient for different hydro-erosive grinding levels for nozzle 105

HEG time	0	20	40	60	80	100	120	140
AVG Cd	0.583	0.713	0.728	0.742	0.752	0.763	0.775	0.791
Improvement	0	22%	25%	27%	29%	31%	33%	36%

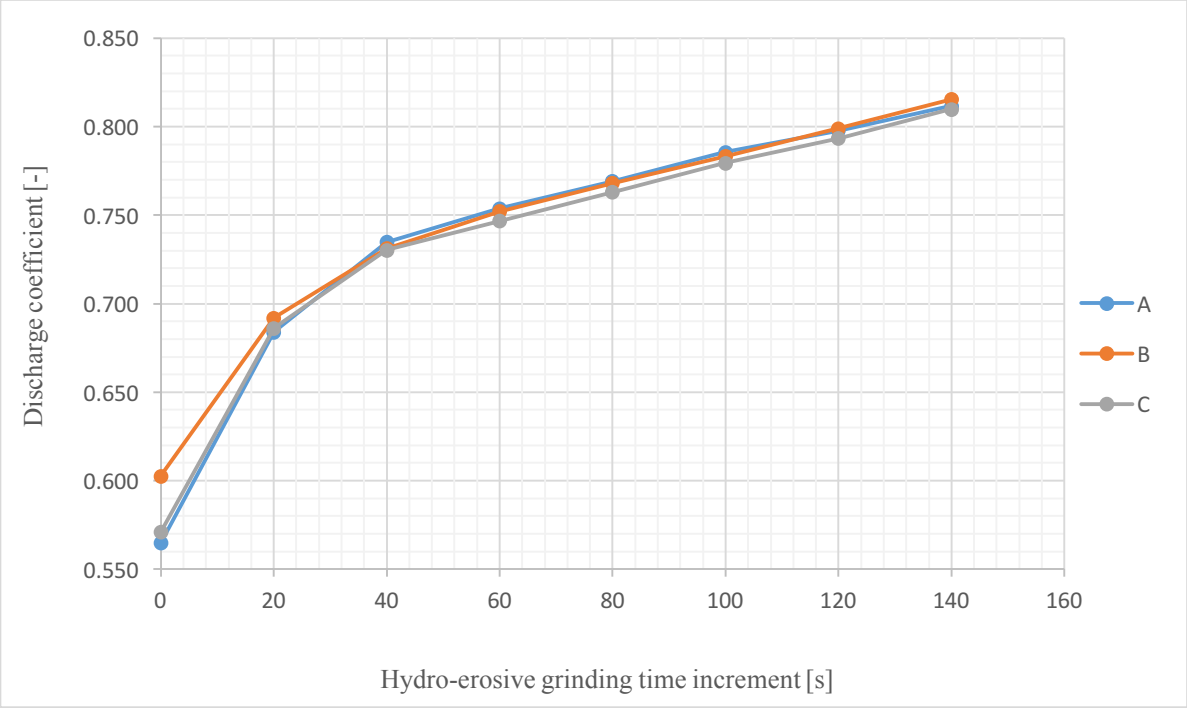

Figure 3.16 Measured discharge coefficient for different hydro-erosive grinding levels for nozzles type 104

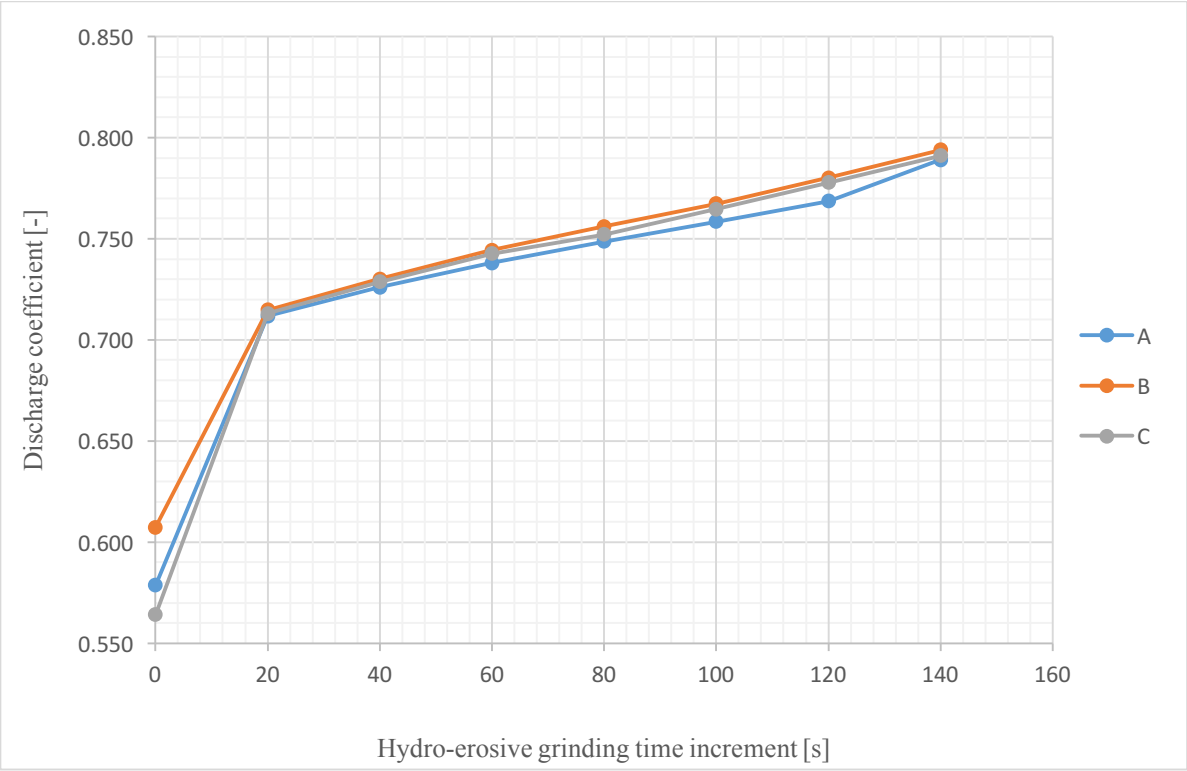

Figure 3.17 Measured discharge coefficient for different hydro-erosive grinding levels for nozzles type 105

3.5.4 Comparison of three types of nozzles

In Figure 3.18 the average discharge coefficient of all three types of nozzles is shown for different hydro-erosive grinding levels. As can be seen, nozzle 104 shows slightly different behavior in comparison with the other types. The growth rate in the discharge coefficient of nozzle 104 is slower at the beginning until it becomes linear. In addition, after 140 s of hydro-erosive grinding, it provides the highest discharge coefficient. Therefore, it can be said that the orifices which are tangential to the nozzle suffer more about sharp edges at the entrance of the orifice and hydro-erosive grinding will be more effective in this case. Figure 3.19 illustrates the top cross section of the nozzle 104 before and after hydro-erosive grinding to better understand how the geometry of the nozzle is changed by hydro-erosive grinding.

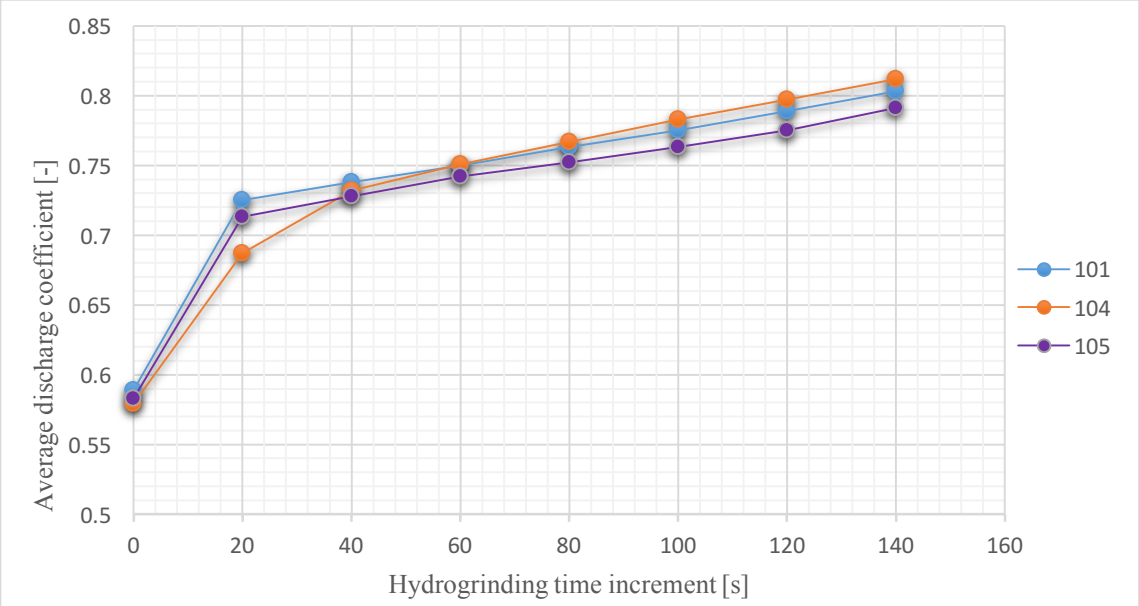

Figure 3.18 Average discharge coefficient for three types of nozzles as a function of hydro-erosive grinding

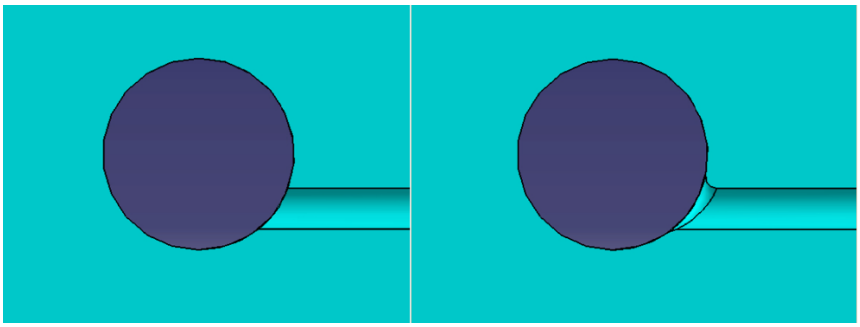

Figure 3. 19 The effect of hydro-erosive grinding on nozzle geometry for nozzle 104

On the other hand, comparing nozzle 101 and 105 shows that both of them has the same trend in increasing of their discharge coefficient over hydro-erosive grinding. However, nozzle 105 which its orifice is angled, is not affected by hydro-erosive grinding as much as nozzle 101 does. It can be concluded that hydro-erosive grinding has less influence on the discharge coefficient of angled orifices. The reason can be explained by less restriction in the flow pathway on angled orifices. Figure 3.20 is good reference in order to better understand this difference. As can be seen, deflection in the straight orifice cause higher resistance for the flow in comparison with angled orifice.

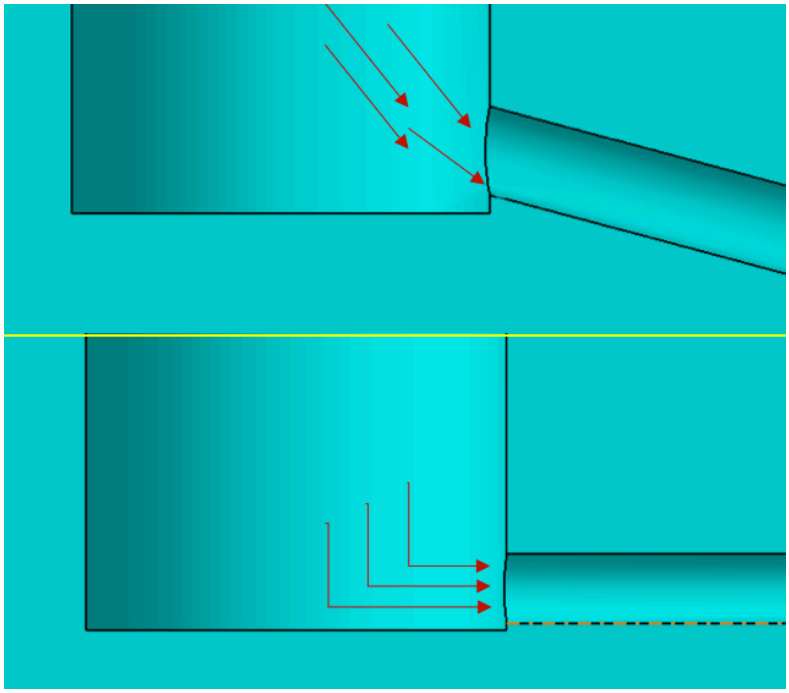

Figure 3. 20 Comparing flow inside straight and angles orifices

The features mentioned above are more sensible if the percentage of increase in discharge coefficient is calculated respect the standard nozzle. In Figure 3.21 the percentage of increase in the discharge coefficient is plotted for different nozzles under different hydro-erosive grinding levels. In this figure, different behaviors of different nozzles are more obvious. For instance, in the linear part of the plot, nozzle 104 seems to have slightly higher slop comparing to the other types.

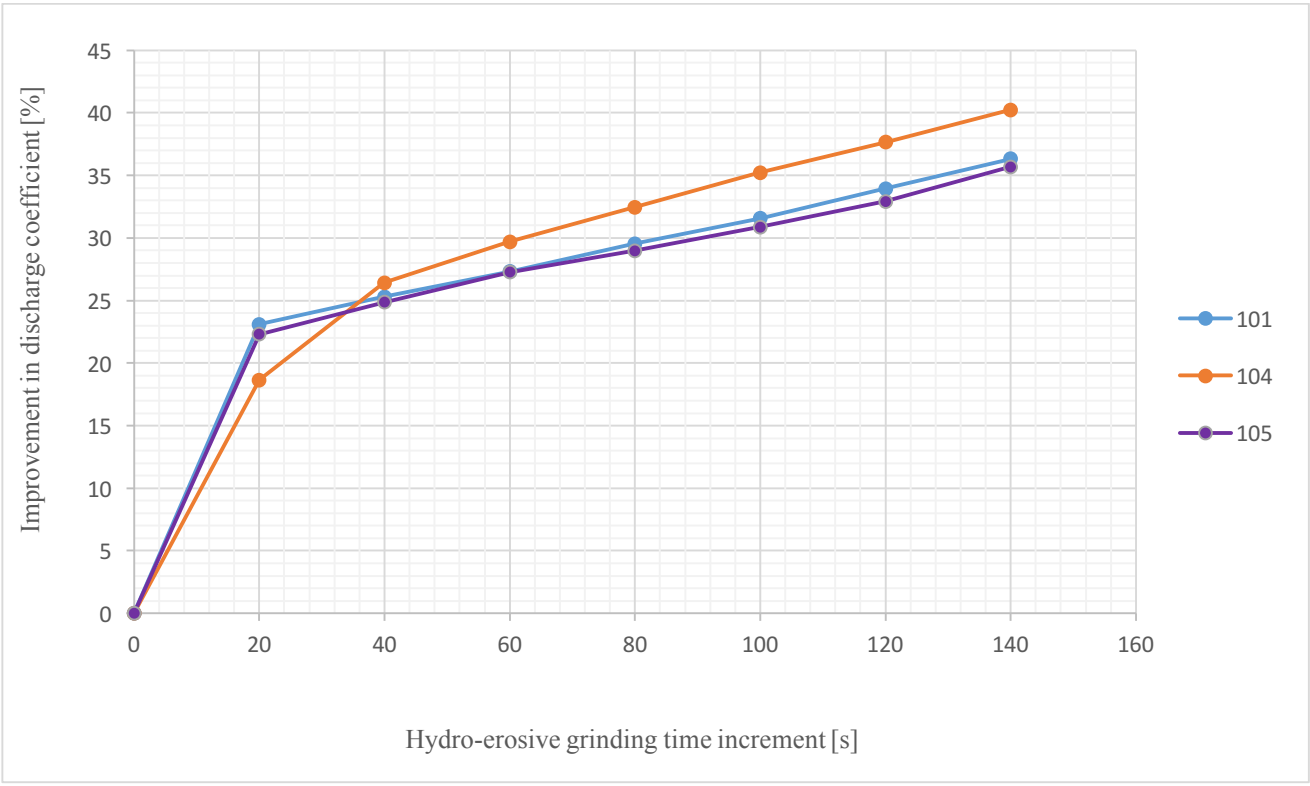

Figure 3.21 Improvement in discharge coefficient for three types of nozzles

3.5.5 An important note

Referring to the results of another research which observes cavitation formation inside the same nozzles at the same hydro-erosive grinding conditions, cavitation is vanished after performing 120 s of hydro-erosive grinding and it is expected that the trend of increasing discharge coefficient converges after this point [1]. However, it seems that it increases linearly even after 140 s of hydro-erosive grinding. One of the possible reasons to explain this contradiction is that hydro-erosive grinding does not only round sharp edges but also it removes a very thin layer of the surface wall. Although the thickness of this layer is negligible but it affects cross sectional area which provides higher mass flow rate. According to Equation (3.1), at the same pressure difference and same mass flow rate, smaller area will have higher discharge coefficient. In another words, with the same cross sectional area and at the same pressure difference, higher mass flow rate represents higher discharge coefficient. However, it should be noticed that this marginal higher mass flow rate comes from marginal larger cross sectional area which is made by hydro-erosive grinding.

Chapter 4

4. Conclusion

4.1 Results from present work

The results show that hydro-erosive grinding can be considered as a suitable solution to reduce cavitation inside the injector nozzle and its orifices. It also causes a considerable increase in the discharge coefficient of the nozzle orifices and therefore, losses in fuel injection is decreased.

As can be seen in Figures 3.15 to 3.17, the first increment (20 s) of hydro-erosive grinding has the highest impact on the discharge coefficient while for nozzle 104, two increments (40 s) should be applied to have the same level of discharge coefficient.

It also can be concluded that cavitation phenomenon is more prone to occur as the nozzle orifice moves from center to the tangential position of the nozzle tip and higher loss can be observed in the injected flow. Therefore, hydro-erosive grinding has the highest impact on these types of nozzles. On the other hand, inclination in nozzle orifices facilitates flow motion at the entrance of the orifice and hinders cavitation at that point. This is a reason which explains lower impact of hydro-erosive grinding on discharge coefficient improvement in angled orifices.

4.2 Future work

As a very important note which is mentioned in Section 3.5.5, although the impact of hydro-erosive grinding on cross-sectional area is not significant, however it is highly recommended to investigate the accurate amount of increase in cross-sectional area after each hydro-erosive increment and make correction on the obtained results by this thesis project.

In addition, it is advised to calculate the efficiency of this type of grinding and compare it to the other types of accurate machining methods to find out the best situation for rounding sharp edges of the orifice in terms of time, cost and energy consumption.

Finally, the last suggestion is to investigate the effects of variation in hydro-erosive parameters such as pressure and abrasive media properties on surface removing and specially, on rounding sharp edges.

References

[1]. R. Balz "In-nozzle flow and primary breakup investigations of marine two-stroke diesel engine injectors," Licentiate Thesis, Dept. Mechanics and Maritime Science, Chalmers University of Technology, 2018

[2]. F. M. White, "Fluid Mechanics," 7th Edition, Mc Graw Hill, New York, NY 10020, 2011

[3]. IET Institute for Energy Technology [online], https://www.youtube.com/watch?v=U-uUYCFDTrc [Accessed March 2018]

[4]. [Online], http://top-mechanics.blogfa.com/post-15.aspx [Accessed March 2018]

[5]. F. Payri, R. Payri, F.J. Salvador, J. Martínez-López, "A contribution to the understanding of cavitation effects in diesel injector nozzles through a combined experimental and computational investigation, Computers & Fluids," 58 (2012) 88–101

[6]. J. Javier López, F.J. Salvador, O. A. de la Garza, J. Arrègle, "A comprehensive study on the effect of cavitation on injection velocity in diesel nozzles," Energy Conversion and Management 64 (2012) 415–423

[7]. Z.Y. Sun, G.X. Li ⇑, C. Chen, Y.S. Yu, G.X. Gao, "Numerical investigation on effects of nozzle's geometric parameters on the flow and the cavitation characteristics within injector's nozzle for a high-pressure common-rail DI diesel engine," Energy Conversion and Management 89 (2015) 843–861

[8]. F. Yan, Y. Du, L. Wang, W. Tang, J. Zhang, B. Liu, C. Liu, "Effects of injection pressure on cavitation and spray in marine diesel engine," International Journal of Spray and Combustion Dynamics 2017, Vol. 9(3) 186–198

[9]. S.Kumar S., S. S. Hiremath, "A Review on Abrasive Flow Machining (AFM)," Procedia Technology 25 (2016) 1297 - 1304

[10]. C. Diver, J. Atkinson, B. Befrui, H. J. Helml, L. Li, "Improving the geometry and quality of a micro-hole fuel injection nozzle by means of hydroerosive grinding," IMechE 221 (2007) Part B: J. Engineering Manufacture

[11]. F.J. Salvador, M. Carreres, D. Jaramillo, J. Martínez-López, "Analysis of the combined effect of hydrogrinding process and inclination angle on hydraulic performance of diesel injection nozzles," Energy Conversion and Management 105 (2015) 1352–1365

[12]. B. Yu, P.F. Fu, T. Zhang, H-C. Zhou, "The influence of back pressure on the flow discharge coefficients of plain orifice nozzle," International Journal of Heat and Fluid Flow 44 (2013) 509–514

[13]. A. Motazedi-Fard, "Fundamentals of Measurement and Error Calculation", The Physics Society of Iran, 2015.